# The Functionalisation of Electrospun Polymer Scaffolds Using Natural Peptides

Student Name: Jeremy Eastwood-Smith

Registration No.: B00695171

Module Code: BME503

Course Title: BSc Biomedical Engineering

Supervisor:  Dr George Burke

**School of Engineering**

**Faculty of Computing and Engineering**

**2018/19**

# Acknowledgements

# Summary

Biomedical scaffolds are designed to modify or support tissue repair and growth during wound healing. Using a biodegradable synthetic polymer of L-lactide and ε-caprolactone copolymer, scaffolds are electrospun to create a thin material of non-woven fibers, with a high surface area. The degradation of the material will mean that the material can be resorbed without the need for surgical removal, and the high surface area and porosity cells should be able to grow and proliferate across and inside the scaffold matrix. However, synthetic polymers have few biological cues that cells could attach to, the polymer surface needs to be made more receptive to cells by adsorbing peptide sequences to the material. Some specific sequences, ligands, interact with adhesion molecules in the surface of the cells, integrins, and these molecules signal cells to adhere or move depending on the specific integrins and ligand sequence.  Peptides tend to be polar, due to the acidic and basic groups, meaning they may not adsorb to the surface of a non-polar polymer. To improve the wettability of the scaffolds, dielectric barrier discharge (DBD) plasma is used to create polar groups on the fiber surfaces to increase hydrogen bonding. Plasma applies energy to the material, and the thin fibers of the scaffolds absorb that energy, damaging the material generating changes in the surface and network of the fibers. 500 Watts of plasma power was found to be an acceptable compromise between topography, hydrophilicity and fiber network damage.

A cell nutrient mixture full of protein and growth factors was adhered to the surface of the polymer scaffolds, and the DBD treatment was tested for efficacy. Confocal fluorescent images prove that albumin binds to both the treated and untreated scaffolds. However, since no quantitative analysis was performed the relationship between DBD treatment and peptide adsorption was not established

# Table of Contents

# List of Figures

# List of Tables and Graphs

# Nomenclature

All variable listed in alphabetical order, including Greek letters.

| | |
|---|---|
| *ATR-FTIR* | Attenuated Total Reflected Fourier Transform InfraRed spectroscopy technique |
| *BCA* | Bicinchoninic acid |
| *BSA* | Bovine Serum Albumin |
| *C* | Carbon atom |
| *DBD* | Dielectric Barrier Discharge |
| *DMF* | Dimethyl Formamide |
| *ECM* | Extra Cellular Matrix |
| *ε* | Epsilon, one isomer of caprolactone |
| *FBS* | Foetal Bovine Serum |
| *U.S. FDA* | United States Food and Drug Administration |
| *H* | Hydrogen atom |
| *IMS* | Industrial Methylated Spirits |
| *μ* | Mu, Micro x$10^{-6}$ |
| *N* | Nitrogen atom |
| *O* | Oxygen atom |
| *PLCL* | Poly(L-lactide-ε-co-caprolactone) |
| *PLGA* | Poly(Lactic-co-glycolic acid) |
| *RGD* | Arginyl-Glycyl-Aspartic acid, peptide sequence |
| *SEM* | Scanning Electron Microscope |
| *σ* | Sigma, Standard Deviation |
| *TFBA* | 4-(Trifluoromethyl) benzaldehyde |
| *W* | Watts, unit of power |
| *XPS* | X-ray Photoelectric Spectroscopy |
| *C-C* | Single bond between two carbon atoms |
| *C=O* | Double bond between Carbon and Oxygen atoms |

# Chapter 1. **Introduction**

## 1.1    **Introduction**

Tissue engineering is a method of repairing or modifying cell proliferation by using engineered materials and chemical interactions to design the cellular response for a particular function. Electrospinning is a versatile technique that is gaining popularity with tissue engineers (Varesano, 2015, Augustine *et al.*, 2015, Bridge et at., 2015, Christopherson *et al.*, 2009 and Pham *et al.* 2009) because many soluble polymers can be produced inexpensively into a thin mesh with a large surface area. These methods can be scaled up for production and specified with specialty nozzles (Varesano, 2015) to produce compound fibers. The structures created in the spinning process can be random, self-assembling or aligned in orientation of the electric field of the collector allowing enormous variation in the possible products of the technique. Fibrous structures mimicking the extracellular structures creating connective tissue would encourage appropriate cell differentiation and response.

The surface characteristics of a biocompatible material affect how cells will interact with the material (Kerr 2011). Protein adsorption would make for a more adhesive surface for cell adherence; however, this same adhesive interaction could interfere with the platelets of the blood in the cardiovascular system, creating thromboses (Boyce *et al.*, 1983). Therefore, functionalization treatment must be designed with the tissue's function in mind as one method will not be suitable for all tissue engineering applications, instead the tissue repair and regrowth by the transport of pluripotent stem cells on an appropriately functionalised scaffold that recruits host cells (Ko *et al.*, 2012).

The methods of functionalization can take many forms as described by Tallawi *et al.*, (2015) and Bridge *et al.*, (2015): Different molecules like growth factors or extracellular matrix proteins (ECM) applied to materials before or after production have varying resulting characteristics depending on the chosen molecules. Surface modification with plasma or chemical treatment is used to incorporate biological cues or reactive groups into the manufacturing process or imprinting a selected molecule to the material to elicit a specific response. The plan for this project is a mix of covalent bonding and adsorption of the peptide molecules like arginyl-glycyl-aspartic acid (RGD) to plasma grafted carboxyl groups on the scaffolds, to mimic the extracellular matrix with bio cues that cells can interact with. However, complications with the grafting and polymerisation process may make covalent bonding unachievable. As a contingency, only adsorbing the peptide to the DBD plasma treated

scaffolds will result in improved cell adhesion providing there are enough functional groups on the material.

# Chapter 2. **Literature Review**

Electrospun biodegradable polymers are emerging as a viable way to transport differentiated cells to a patient for tissue engineering. The organic polymers have low hydrophilicity since they are comprised of a long carbon backbone with mostly non-polar groups on either side of the chain, so the molecule is relatively non-polar compared to water. Poly(L-lactide-co-ε-caprolactone) (PLCL) has many ester bonds which will make it more hydrophilic than a straight-chained polymer like polyethylene, due to the greater dipole moment of carbon oxygen bonds compared to carbon hydrogen bonds, increasing the relative polarity of the polyester. Functionalising the polymer scaffolds with dielectric barrier discharge (DBD) plasma under atmospheric pressure will increase the functional group density and distribution over the scaffold improving the materials' hydrophilicity. Peptides adsorb to hydrophilic surfaces because they too are hydrophilic and so, form hydrogen bonds with polar groups that will be more concentrated on the DBD treated scaffolds. As well the DBD plasma treatment will create living radicals on the surface of the scaffold where amine groups of peptides could be bonded to, but DBD plasma treatment of the polymer scaffold and RGD peptide monomers together may result in rapid and uncontrolled cross-linking creating a coagulated peptide mass.

## 2.1    Research Objectives

Research in the area suggests that peptides or proteins can be bonded to materials to improve their cellular interactions using a variety of techniques. Different techniques have their benefits and limitations, for example binding collagen to the surface of PCL is more effectively achieved when grafting acrylic molecules to the surface, presenting carboxyl groups for peptide bonding with multiple production steps. Therefore, the most general method should be chosen to functionalise generic electrospun polymer, evaluate currently used methods by scientists and modify it to streamline functionalisation.

The understanding of the factors of a material's surface that affect cellular response like topography and surface free energy will educate observations made during the project. How these properties will be affected by adsorption must be understood before applying the knowledge to tissue engineering and regenerative medicine (TERM) scaffolds.

## 2.2   Electrospinning

The process of depositing thin fibers by charging them with electricity, stretching the intermolecular bonds of a polymer in solution between two oppositely charged electrodes. While the jet extends from the needle tip the liquid filament flies straight towards the collector, evaporating solvent as it travels and begins to whip in convective flow. This method produces a non-woven mesh of filaments 2 or 3-dimensional structures with specialised micro and nano-topography. Electrospun material has a large surface area to volume ratio as a result of the network of fibers making them ideal for cell growth by mimicking the extracellular matrix. Using biodegradable polymers to produce these fiber matrices can improve the patients experience with the product. Since internal and external tissue engineering cell vectors will degrade into useful metabolites that are resorbed by the body, eliminating the need for removal surgery.

### 2.2.1 Parameters

Leach *et al.*, (2011) discuss many parameters that affect the mechanics of the electrospinning process including voltage difference between the needle and collector plate as well as the distance separating them. The paper discusses the factors involved in bead formation and fiber alignment, as well as explaining how to go from solution to set-up troubleshooting remedies for common problems. Cramariuc *et al.*, (2013) mention the diameter of the fibers can be predicted using formulae that suggest fiber diameter is mostly a factor of current applied, flow rate and surface tension of the solution.

*Polymer Solution*

As well, the solution used for spinning plays a crucial role, since the volatility of the solvents used will change the distance at which the polymer strand begins convective flow (Leach *et al.*, 2011). If the polymer solution cannot conduct enough voltage or the collector potential difference is insufficient the polymer does not electrostatically stream across the distance, but flicker from a bead at the needle tip, but a speckled mass of unusable polymer.

PLCL is a biodegradable polymer that is hydrolytically cleaved into L-Lactide which will convert into lactic acid and 6-Hydroxyhaxanoic acid. Both breakdown products are acidic and so will reduce the pH of the surrounding tissue, meaning the rate of polymer degradation must be modifiable to allow diffusion of acidic metabolites and not damage surrounding tissue.

The polymer is dissolved in chloroform and dimethylformamide (DMF) in a ratio of 8 to 2 because chloroform has a boiling point of 61.2 degrees, so it evaporates out of solution when spun. DMF has a boiling point higher than water, 153 degrees and so according to Leach *et al*.

(2011) this will produce less porous fibers. Adjusting the concentrations of the polymer and the ratios of the solvents used will result in differing surface characteristics, resulting in an unacceptable variation in the polymer scaffolds.

As discussed by Larrañaga *et al.*, (2014), PLCL can hydrolytically degrade reducing the polymers elastic properties, which is an important consideration for a tissue engineering scaffold intended for use in mobile tissue. The paper mentions a mixture of 66.9% L-lactide, 17.4% D-lactide and 15.7% ε-caprolactone has reduced degradation and crystallisation over a 98-day hydrolytic degradation study, due to shorter sequence lengths on average. The reduced degradation profile suggests PLCL will be stable for long periods in the body and could be used for long term treatments or healing. PCL degrades over years in the body (Gao *et al.*, 2018) and so the degradation rate can be altered by proportion of caprolactone copolymer.

## 2.2.2 Taylor Cone Theory

Sir Geoffrey Taylor noticed that there was a predictable shape produced when the surface tension of a droplet reaches equilibrium with the electrostatic forces applied by a high voltage (Varesano 2015). When the electrostatic forces are increased to the critical potential overcoming equilibrium, the liquid body forms into a cone with an angle of 98.6 degrees. To find the operating voltages for the electrospinner, using the equation below:

$$V_c = 4\frac{H^2}{L^2}\left(ln\frac{2L}{R} - \frac{3}{2}\right)(0.117\pi\gamma R)$$

Where $V_c$ is the voltage, H is the distance between the needle and collector, L is the length and R is the diameter of the syringe and $\gamma$ is the surface tension of the solution (Gittsegrad 2018).

## 2.2.3 Scaffolds

Electrostatic interactions between deposited and in-flight fibers and the collector plate architecture affect deposition (Varesano 2015). Filaments can be influenced to align themselves randomly on a flat stationary plate, parallel on a rotating drum or wheel, or in the geometry of a patterned collector plate.

Since this project is not targeted towards a particular cell type, random deposition electrospinning will be sufficient to experiment with the functionalisation. And yield useful results for generic tissue remodelling, this data should provide a base for more selective tissue applications. The diameter and uniformity of the polymer strands deposited at the collector plate is a quality control measure for the scaffolds produced. If there is too much variation between

polymer fiber diameters, or there are many topographical variations the scaffold will not be evenly treated by the atmospheric plasma, which will affect the distribution of cells on the scaffold.

## 2.2.4 Controls

The use of controls is vital in the scientific method because there must be non-trivial evidence that the parameter that is being tested is the only factor that changes, i.e., the difference in the results are due to the modification of the experimental parameter. Therefore, the physical and chemical characteristics of the scaffolds must be determined with sufficient data points. These characteristics must be shown not to stray significantly from the regulatory standards after DBD plasma treatment.

## 2.2.5  Rotating Mandrel

At low voltages applied to the motor of a rotating mandrel, the mandrel spins slowly (< 100rpm) allowing fibers to arrange themselves randomly (Bridge *et al*., 2015 and Varesano 2015). The rotation produces fiber mesh samples with a more even thickness than those produced by a stationary collector plate. In conjunction with being a less variable production method, the scaffolds produced on a rotating mandrel are more reliable and reproducible. Using an rpm of 2000 produces aligned fibers, which would be preferred by ligament fibroblasts as evidenced by Subramony *et al*., (2013) where the mechanical loading of Mesenchymal stem cells on aligned fibers stimulates differentiation to fibroblast-like cells.

## 2.3    Characterisation

There exist many ways to characterise the properties of a material, including the mechanical strength under tension, compression or shear, the thermal properties or chemistry of a material. Biocompatibility mostly depends on the physical and chemical interactions between the materials and colonising cells, for example, a hydrophilic material will (in principle) interact well with hydrophilic proteins. Hydrophilicity could be considered a physical or chemical characteristic of a property because it is a result of the bond interactions between polar molecules like water and the material's surface, which can be affected by porosity since the angle of the material boundaries changes with topography.

## 2.3.1 Physical Characterisation Methods

*Sessile Drop Contact Angle Analysis*

When a 5 µL droplet of liquid is applied to a surface, depending on the surface energy of the material, the angle between the surface and the edge of the bead of the water can be

related using Young-Laplace equation. (Grumezescu, 2017) Relatively high energy surfaces form more hydrogen bonds with the water molecules and overcome the surface tension of the droplet decreasing the contact angle. The gravitational forces on the droplet can be considered negligible because of the size of the droplet. Therefore, the hydrophilicity of the surface can be measured using a simple apparatus that images a known quantity of polar liquid (often water) deposited on the scaffold and the angle determined by a computer, providing an accurate assessment.

Electrospun meshes are porous, and their surfaces are uneven which means the fluid tends to take longer to stabilise on the material which can make measuring the contact angle using water a challenge. Bostwick (2009) suggests that it is the viscosity, not surface tension of a liquid that determines the duration of inertial wetting. Possibly due to viscous damping, this means that a viscous and polar fluid like glycerol will spread more slowly across the surface and have a more stable angle over time.

**Young's Equation**

The three-phase boundary between the glycerol droplet, the air and the scaffold surface using the equation below:

$$\gamma_s = \gamma_{sl} + \gamma_l cos\theta$$

Where $\gamma_l$ is the surface tension of the liquid phase, $\gamma_{sl}$ is the interface tension between the liquid and solid, $\gamma_s$ is the free energy of the surface and θ is the angle where the liquid-air interface intersects the solid-liquid interface. Hejda, Solăr, Kousal (2010) suggest that using various liquids better allows for variability from vapour absorption and pressure spreading to affect the work adhesion calculation. There is a challenge in measuring contact angle over a porous material as the liquid can diffuse through the spaces, changing the volume of the drop, which will change the angle of the interface.

*Scanning Electron Microscopy*

Passing electrons in a directed beam over the electrically conductive surface of a sample, the reflected electrons and X-rays build up a picture of the surface topography. The scanning electron microscope (SEM) images have a resolution of around 4nm and so can be used to measure the thickness of the polymer strands in the sample. Statistics software like ImageJ (National Institutes of Health, Bethesda U.S.) can be used to determine if the filaments produced in the scaffolds are statistically acceptable.

The porosity of the scaffolds will influence the nutrient exchange, improving or restricting the removal of the metabolic waste of the cells of the tissue. The pores in the scaffold can be seen on the SEM machine, but the superficiality of the pores cannot be accurately represented, so pore dimensions generated by ImageJ are expected to be of little use.

The topography of the PLCL fibers can also be visually represented, but the texture and cellular response are not measurable with this technology. Atomic Force Microscopy (AFM) would be more effective at evaluating the texture as it can measure the depth and variation of the nanoscopic structures. PLCL is an insulating material and so can only be measured by tapping-mode AFM, where the needle beats against the surface and the intermolecular forces between the needle and fiber are measured (Payton *et al.*, 2010).

Scaffold topography and alignment is integral to cell selection, randomly aligned fibers are more likely to facilitate the development of non-directional cells like squamous or columnar epithelial tissue, whereas an aligned scaffold would be a better surface for myocytes. Using a flow perfusion bioreactor with randomly aligned scaffolds stacked 100 μm apart with thicker scaffolds to segment skeletal muscle cells, could allow myocyte growth as a three dimensional tissue. With a PCL aligned fiber tube encircling all of the z-disks along the length of the muscle fiber that would represent the basal lamina, since poly(caprolactone) has longitudinal ridges when electrospun that could encourage myotube formation (Varesano 2015). Possibly mixing polyaniline into the mixture to improve formation of satellite cells, as done by Mahmoudifard *et al.*, (2016) using polyaniline and polyacrylonitile for their conductivity that better supports the growth of muscle tissue. Jun, Jeong and Shin, (2009) found myoblasts differentiate into satellite cells on PLCL/polyaniline composite electrospun scaffolds, thanks to their electrical cues.

## 2.3.2 Chemical Characterisation

*Fourier Transform Infrared Spectroscopy*

Chemical bonds between atoms are not mechanically rigid structures of a molecule but an electrostatic attraction of the positively charged nuclei and local electrons. When there is an uneven distribution of charge across the atoms of a molecule, a dipole moment, the bonds can selectively absorb infrared (IR) energy (Royal Society of Chemistry, 2009). The energy each bond can absorb is dependent on the light's frequency matching the energy difference between the ground and excited state of the bond. By measuring the absorption of radiation by the material for each wavenumber in the IR spectrum, the chemical bonds present in the material can be predicted by comparing the frequency spectrum to a database of bond absorption spectrums.

Attenuated Total Reflectance Fourier Transform Infrared spectroscopy, or FTIR for short, is a qualitative technique not quantitative, meaning it can only be used to determine the types of bonds of the material and not the absolute number of bonds. An FTIR spectrum of the control PLCL scaffold controls should show the existence of ester bonds between the L-lactide and the ε-caprolactone, whereas oxidation due to DBD plasma treatment in atmospheric gas will show carboxylic acid, ketone and hydroxyl groups (Tallawi *et al.*, 2015).

*Protein Estimation*

Bicinchoninic acid (BCA) assay is a method of measuring protein quantities by the absorption of 562nm light due to the reduction of $Cu^{2+}$ to $Cu^{1+}$ ions of the BCA reagent at peptide bonds in the RGD (Sirsi 2014). Using a spectrophotometer along with BCA or fluorescamine the measured absorbance of the relevant wavelengths will be useful to show the relative quantity of peptide bonding. Fluorescein bonds to free amine groups which are present in RGD, during the polymerisation process, however, these side chain amine groups could react with carboxyl groups meaning the resulting spectrograph would not necessarily correspond to any 1 to 1 fluorophore calibration graphs. The working range of the BCA assay is between 20 and 2000 µg/ml (Johnson, 2012), since the adsorption is unknown and presumed as a protein monolayer, the quantity of protein may be beneath the working range.

4-(Trifluoromethyl)benzaldehyde (TFBA) was used by Larrañaga *et al.* (2014) to quantify amino acids on a surface because azomethines form between the aldehyde group of TFBA and amine groups (NH2), that are only present in the amino acids. XPS confirms the presence of fluorine, and the material showed approximately 0.5% surface amine groups. The uses of TFBA in solution must be evaluated by safety officers and industrial hygienists familiar with the intended application, and so it is not applicable to a final year project.

*Detergent*

By attempting to remove the peptides using a mixture of ionic and non-ionic solvents and re-measuring the peptide content, the change in absorbed light would represent the RGD-fluorescein that is weakly bonded to the surface (MacDonal et al., 2008). The strength of the bonding will correlate with the adhesion of cells, because (weakly)

adsorbed markers may wash away during production or cell culturing processes, reducing the cellular adhesion.

*Confocal Microscopy*

An imaging technique achieved by focusing a LASER through dichromic mirrors, lenses and filters to excite fluorophores at different focal planes in the sample. The light is reflected through the filters and lenses removing UV radiation before the fluorescent light is seen in the eyepiece or camera. This technique can be used to visualise intrinsic fluorescence in material, protein adherence to surfaces and cellular structure when organelles and proteins are bonded to fluorescently conjugated immunoglobulin. The fluorophores are excited within a few nanometres of the position of the target substance and so can give a detailed view of the structures of a cell, and so have a built-in inaccuracy of at least two times the length of the immunoglobulin, 9.3 nm *2 = 18.6 nm (Pease *et al*,. 2008). This inherent downside of indirect immunofluorescence is negligible at the scale of this project, and so is not a concern.

## 2.4    Plasma Treatment

Plasma is a gaseous mixture of anions and electrons which can be formed under high energy and voltage conditions in high- or low-pressure systems. Plasma is categorised by the temperature of the non-ionised gas particles, in near-equilibrium or hot plasma the electrons have collided with neutral particles to the extent that they both have similar energy. In a cold-plasma, the electrons have significantly more energy than the neutral species, often because the pressure is low and there are not many collisions distributing the thermal energy of the electrons.

The ionised gas molecules form radicals, these ionise the surface of the polymer or the material being treated, creating or binding radicals to the surface increasing the free energy of the surface. These reactive areas can electrostatically interact with species in the medium or gas and create functional groups on the polymer surface like carboxyl and alcohol groups in atmospheric pressure in the DBD chamber. By limiting the duration of the treatment, the bulk properties of the material remain unchanged and if the Fourier transform infrared (FTIR) analysis retains the fingerprint of PLCL these modified polymers may still be considered a medically viable material that wouldn't require separate clinical trials.

### 2.4.1 Set-Up

As Kerr (2011, p. 16) argues, the configuration of the DBD system will vary the effect of the treatment on the polymer, so there must be a protocol based on the degree of modification that will achieve the desired effect to the surface. Electrode gap, plasma exposure time and the power discharged are some of the variables that will have to be tuned to achieve the desired surface wettability of the polymer. Tallawi *et al.*, (2015) found that just 2 minutes of DBD plasma treatment could improve the hydrophilicity of a surface from a contact angle of 78 to 45 degrees, which would improve peptide and cell adsorption.

As referred to by Kerr (2011, p.19) the dielectric material chosen can affect the surface modification, where a quartz electrode generates random filamentary discharge that generates more stable oxidised surfaces. Metal electrodes more uniformly treated the surface of the scaffold, improving the hydrophilicity by generating a consistently polarised surface. The stability of the scaffolds can be altered with polymer composition, so the uniformity generated by the metal electrodes is a more desirable result.

### 2.4.2 Chemical Interactions

Rehman *et al.*, (2016) discusses the formation of radicals and ions in atmospheric non-thermal plasma. Mentioning argon and helium plasmas are most often used because they produce stable plasma but other gasses can be used to form different reactive species. Amine groups could be bound to the surface if nitrogen and hydrogen gas are pumped in.

Werthiemer *et al.* (1999) discussed the production of carboxyl groups in oxygen-containing low energy plasma within seconds of treatment, meaning surface modifications will include carboxyl grafting. The free-radical pathways described in the paper include mechanisms for carboxyl groups to form on the surface and which could be used to covalently bond molecules like RGD or albumin to the polymer surface. This suggests that secondary plasma treatment with a solution of RGD or Albumin may bond to the polymer and polymerise more peptide bonds by propagating radical production.

### 2.4.3 Intermediary Chemicals

Kerr's (2011, p. 28) thesis mentions that there must be enough spacing between the grafted functional groups, or else bonded molecules may block functional groups. By overcrowding, the surface bioactivity can be diminished by the excess of groups that would overlap resulting in an over functionalised surface. Acrylic is a simple monomer that would readily bind to the surface of PCL under DBD, grafting a carboxyl group for the amine groups of

RGD to bind. At the cost of another manufacturing process the benefit of this would be better reactivity of the ketone groups in the PLCL fibers, but whether or not the spacing would make a significant difference to the formation of an RGD coating is unknown. Tallawi *et al.*, (2015) claims in section 2.1.6 that an RGD coating results in a "disorganized cyto-architecture" meaning specific surfaces may be hindered by the random adsorption or bonding of RGD, rendering it useless for the highly ordered cytoskeleton of cardiac tissue for example.

If the functional groups formed by the initial plasma treatment step do not include carboxyl groups, there may be too much bond enthalpy in ester bonds to destabilise the hydroxyl group that form the peptide bonds. If this is the case, the double carbon bond in acrylic could be disrupted by the radicals of the plasma and bond to a reactive area of the polymer surface, resulting with the carboxyl group being presented for the condensation reaction to occur.

### 2.4.4 Polymeric Scissions

The separation of polymeric backbone bonds in the material by hydrogen and oxygen-containing radical groups results in a radical electron on one end of the broken chain and a functional group on the other. This radical atom could bond to another radical in a functional group or polymer chain terminating the radical propagation (Grüven 1990).

### 2.4.5 Uniformity of Treatment

The uniformity of the plasma treatment is affected by many factors like the dielectric material used for the electrodes, and as discussed by Lauer *et al.* (2005) the size of the chamber can affect the discharge of the plasma, Kerr (2011) suggested metal elctrodes have an improved uniformity over ceramic. A large chamber (and electrodes) will result in more charge close to the electrode connectors, and so in larger machines there can be microelectrodes installed distributing the plasma inducing current evenly.

### 2.4.6 Cross-linking

Ends of polymer chains can bond to one another to increase the length of the chain and change the bulk properties by stabilising the polymer. This effect is lessened by the presence of oxygen groups that would be favourably reduced (Grüven 1990).

## 2.5   Functionalisation Using Natural Peptides

### 2.5.1 Foetal Bovine Serum

Foetal Bovine Serum (FBS) is the plasma separated from the clotted blood of foetal calves, centrifuged and filtered to remove the formed elements (red and white blood cells and

platelets), fibrinogen and clotting factors like IgG by not adding anticoagulant. (Van de Valk *et al.*, 2018) It is made up of 38 mg/mL proteins including albumin (23mg/mL) and haemoglobin (113 µg/mL), as well as vitamins, salts, growth factors, hormones like Cholesterol and Progesterone, and metabolites meaning the product can vary lot to lot. Growth factors effect cell differentiation meaning for tissue engineering a serum-free method would need to be adopted to avoid competing differentiation. In addition, FBS can contain heat stable endotoxins (0.35 ng/mL) meaning contamination or systematic inflammatory response syndrome could be induced in the patient in mg quantities.

## 2.5.2 Albumin

Albumin is used as a model protein (Larrañaga *et al.*, 2014) because it is comparatively cheap, however using a protein with a tertiary structure is not going to produce a perfect analogue for repeating RGD peptides. There are no units of RGD in the primary structure of albumin and so cellular integrin interactions will not be analogous, but merely a change in hydrostatic interactions. Proving that peptides adsorb to treated scaffolds because of the functional groups will be useful as a precursor to using a more expensive reagent like RGD.

BSA is used to test adherence because the other characterisation techniques may be uncertain and difficult to interpret, immunocytochemistry is an unmistakable technique. Either there is no protein adhered, resulting in no visible fluorescence or it has adsorbed in which case there will be a florescent fibrous matrix.

## 2.5.3 Integrin interactions

A type of transmembrane protein that is involved with the adhesion of cells to bio-cues on the ECM and other cells. Many integrins on the surface of the cell bind weakly to the specific ligands of an ECM protein, creating adherence by number. Affinity and specificity can be changed by selecting cell specific binding factors that interact with divalent-cation domains of the integrin sub-units (Alberts, 2002). Typically, after an integrin binds to the ligand, the Beta-subunit bind with intracellular anchor proteins forming a complex with actin filaments in the cell, which are associated with motility, eventually in the right conditions integrin clustering will establish a mature focal adhesion.

## 2.5.4 Extra Cellular Matrix

The extracellular matrix is a network of biopolymers that provide anchor points for cell surface integrins, for example collagen and some laminin isoforms expose RGD sequences

after "proteolytic cleavage" (Barczyk, Carracedo and Gullberg, 2009). If the electrospun fibers were coated in these repeating sequences, there would be many of the points for integrin interactions like αVβ1 and α6β1 that maintaining un-differentiation, allowing cell differentiation to be triggered by introducing growth factors at a specified time. Kim (2014) found that inflamed tissue encouraged interstitial migration of effector T cells binding to RGD ligands along the collagen and fibronectin. T cell motility was seen to increase during inflammation meaning this sequence may act to improve immune response for foreign pathogens, reducing infection in the wound area. Laminin specific integrins α7β1 (Tran *et al.*, 2007) are associated with visceral myogenesis.

Electrospun fibers present a cost-effective method of producing ECM mimicking structures like collagen (up to 500nm in diameter Shoulders and Raines, 2009) and elastin (100 nm Payan and Ohayon, 2017). Depending on the operating parameters, fibers with a diameter of 200nm can be spun with variation across diameters introducing variation in the material. The issue is that a synthetic polymer will not have bio cues that stimulate adherence or movement, so by artificially introducing RGD or albumin to the surface should improve cellular interactions (Shen *et al.*, 2015).

The exact composition and proportion of components of the ECM of each tissue type is unknown since external stimuli can cause up-regulation of fibronectin and vitronectin during blood pressure overload in the myocardium (Laser *et al.*, 2000), suggesting signalling pathways can cause changes to the matrix for different tissue functions.

## 2.5.5 RGD

Tallawi (2015) discusses cellular proliferation and differentiation on hydrogels modified with RGD, mentioning that the unmodified hydrogels did not promote cell growth. Suggesting that the presence of the RGD peptide motif in the surface chemistry can drastically improve the cell response to the PLCL scaffolds.

Kerr (2011) states that the concentration of the substrate intended to be grafted affects the distribution of bonding, and saw that a solution of 40% acrylic had the best result under DBD with diminishing returns at higher concentrations. It was found that the substrate had achieved maximum grafting after 3 hours of DBD treatment; this would apply too much energy to the fragile scaffolds damaging the morphology. However grafted oxygen groups are formed under DBD plasma, these groups play a vital role in improving hydrophilicity, but may also provide a chemically reactive site for peptide bonds to form between the PLCL and RGD.

## 2.5.6 Post-treatment

Radicalise the surface of the polymer by DBD treatment under Oxygen or atmospheric conditions to functionalise the material with hydroxyl and oxygen groups and radical zones. Then introduce the peptide that is intended to be bonded to the material and repeat the process, to radicalise the chain ends causing the peptide chain to bond to the radical groups grafted to the PLCL.

## 2.6 Conclusion

Adsorbing peptides directly to the surface of the scaffold will be a simple method that can be reproduced using almost any combination of materials and peptide. Prove that peptides adhere to the fibres by experimenting with a cheap source of protein, developing a method for reliably adhering and testing the samples for contact angle and surface composition. Once a method is successful, experiment with RGD to adhere the peptide to the material and test for contact angle and cellular response.

The response of cells to a bio-cue will depend on the cell types, integrin receptors and the bio-cue itself, but the delicate balance between these factors, growth factor concentrations, topography and mechanical forces to grow the desired tissue is not understood.

# Chapter 3. **Hypothesis and Methodology's**

## 3.1 Project objectives

Create a repeatable protocol to produce scaffolds with statistically similar fiber diameters, pore sizes and thickness. With FTIR analysis ensure no solvent residues are left in the material after electrospinning, since chloroform and DMF are toxic.

Bond peptides to PLCL electrospun scaffolds and determine the effect of 500W DBD treatment on the adsorption of FBS by proving there is peptide bonding on the material by FTIR. Image the distribution of the FBS with confocal Immunocytochemistry (ICC).

Full experimental details including materials and equipment as well as COSCH assessments detailing safety precautions are in the appendices at the end of the document.

## 3.2 Electrospun PLCL Scaffold Production

Electrospin Poly(L-Lactide-ε-Co-Caprolactone) into a thin randomly aligned mesh, with a pore diameter that will accommodate cell proliferation. PLCL is relatively hydrophobic and will resist cell adherence and proliferation on the surface, but the large surface area that results

from many randomly aligned fibers of the scaffold will mimic the extracellular structure providing topography and mechanotransduction.

Electrospinning is a simple process that is very sensitive to environmental conditions, without optimisation of the voltage and the flow rate, the samples can be unacceptably variable due to the Taylor cone growing asymmetrically, spitting beads onto the collector. The horizontal set-up means that gravity can pull a growing Taylor cone down, this is still preferable to a horizontal set-up where the drops are pulled onto the sample by electrostatic and gravitational forces.

## 3.2.1 Methodology

Electrospin PLCL dissolved in 8:2 chloroform to DMF between 16 and 11 kV, with a solution pump rate of 2 mL per hour for 1 hour. Cover the drum of a rotating mandrel with a strip of tin foil to make removal of the sample easy, and apply 2.5 V to the motor to slowly rotate the drum. Adjust the set-up so that the blunt needle is 15 cm from the collector and begin spinning, if the Taylor cone begins to become asymmetrical, open the door and wipe the tip with a paper towel. Gold coat the samples and inspect them under the SEM at 5 kV to better see surface features and topography, analyse the diameters to ensure reproducibility in the samples. Ensure the solvents used in the solution evaporate out of solution during or shortly after electrospinning, since both solvents are toxic and must not be present in the material for tissue engineering.

Previous solvent ratio: 9:1 chloroform to dimethylformamide produced several scaffolds for analysis, the formulation has a high proportion of chloroform which is highly volatile meaning it will rapidly evaporate during the whipping phase of electrospinning. As the solvent evaporates before it reaches the collector, there is less chance of the fibers bleeding into each other (Leach *et al.*, 2011), reducing the available surface area of the scaffold. The less volatile co-solvent DMF produces more even fibers, with few surface pores (Leach *et al.*, 2011).

A solvent ratio of 8:2 chloroform to DMF is simpler to spin and so produces more regular fiber diameters with fewer outliers. The increase of DMF co-solvent will theoretically reduce the porosity of the fibers (Leach *et al.*, 2011) because it is less volatile, however, reliability in sample production is more critical in this phase of the research. A solute of only chloroform would result in porous fibers, affecting the topography of the surface, this solvent

dependant topography will provide a variety of avenues for tailoring the cellular response (Denchai, Tartarini and Mele, 2018).

Previous methodology: The use of a grounded collector plate to produce randomly aligned fibers on 60mm glass cover slides. The manufacturers of the glass slides ceased production, and since the methodology would have to be altered, other techniques for producing random meshes were explored.

The static collector was replaced with a rotating mandrel because the rotation reduces variability in the thickness across the same sample, and at low rotation speeds, the fibers are deposited randomly. The stationary collector would deposit enough material in the centre of the samples, and the perimeter would often have a thinner layer of polymer. But the rotation of the mandrel exposes less insulation between the collector surface and charged needle, and so the electrostatic deposition of the PLCL is more even across the width of the collector area on the mandrel.

## 3.3   Plasma Treatment

Plasma is a gaseous mixture of atoms, cations (positively charged atoms) and electrons generated in high energy environments, for example between high voltage electrodes. Radical species can form in the plasma when a free electron enters an orbital of an atom, ion or molecule as a lone or "valence" electron. Because of these valence electrons, many radical species react more readily with other species. This property can be used to create peroxy (ROO•) radicals on the surface of the scaffolds as well as other oxygen-containing groups. Oxygen and hydrogen form hydrogen bonds with other molecular dipoles, increasing the surface affinity for water and other polar molecules. Improved hydrophilicity means that proteins and peptides will adhere to these treated surfaces, further improving their hydrophilicity. As a result, cellular adherence to the surface will also be improved.

The scaffolds are thin and delicate, applying too much energy to the samples will melt the fibers, causing distortions in the fiber dimensions, morphology and mechanical properties. Therefore, ensuring sample thickness from the electrospinning set-up is important to maintain an experimental thermal mass that will receive a consistent dose of power from the electrodes.

### 3.3.1 Hypothesis

DBD treatment will reduce the contact angle of the polymer scaffolds by increasing the density of high energy groups. Damage to the material will not be sufficient to change the chemical structure, meaning the scaffolds would be biocompatible under PLCL and will not need to be tested for biocompatibility as a different material.

### 3.3.2 Methodology

Remove the spun scaffold from foil backing and place on a non-conductive surface, to be taped to the rubber carriage of the DBD treatment chamber. Apply 250W, 500W, 750W and 1000W of power to electrospun scaffolds in ten machine cycles, at 20% speed, with the electrodes spaced 7.40mm from the electrodes. Evaluate the effect of DBD power on fiber topography using SEM at 5 kV and hydrophilicity by measuring the contact angle of a 5 μL drop of glycerol on the surface of the scaffolds.

## 3.4   Functionalising Scaffolds

Bonding proteins to the surface of the scaffold should increase its hydrophilicity improving interaction with cells, increasing cell proliferation. Hydrogen bonding between albumin and hydroxyl groups of the scaffolds are not strong, meaning the protein could be dislodged by desorption or detergent. Covalently bonding the chemical using radical substitution reactions from the DBD treatment may result in unforeseen reactions and so may not be viable. Grafting side chains to the polymer would allow for covalent bonding at the cost of another manufacturing step. Since adsorption is simple and results would be similar across different polymers, this shall be the method used for this experiment.

### 3.4.1 Hypothesis:

The DBD treated scaffolds with higher surface energy will have an increased adherence by the constituent parts of the FBS compared to the untreated scaffolds because the polar protein molecules would be energetically attracted to the functional groups, increasing hydrogen bonding.

### 3.4.2 Methodology

Prepare 19 mm disks of pristine and 500W DBD treated polymer scaffolds for peptide adherence by sterilisation and rinsing in IMS and de-ionised water. Separate the samples into three groups in a twelve-well plate: pristine control groups for water adsorption, pristine scaffolds for FBS adsorption and DBD treated samples for FBS adsorption, with a plastic ring to

hold the samples to the base of the well plate. Pipette 1mL of FBS into the sample wells, 1mL of de-ionised water for the control, and incubate the samples at 37 ºC overnight. Wash the samples in deionised water, to rinse off unbound protein, and aspirate as much water as possible to speed up the air drying. Compare the contact angle of the samples to evaluate the change in absorptivity. Analyse the FTIR of the samples to prove protein presence and examine the micro-topography of the fibers under SEM.

FTIR spectroscopy can be used to identify chemical bonds present in a sample since the spectrograph of every substance is unique, comparison of the sample to a library of graphs will indicate the bonds present.

## 3.5    Methodology Modifications

Cell study has not begun on these, thus they do not need to be sterilized. However, shrinkage could affect the adsorption of peptide per $mm^2$ since the fibers may contract, tightening the pores.
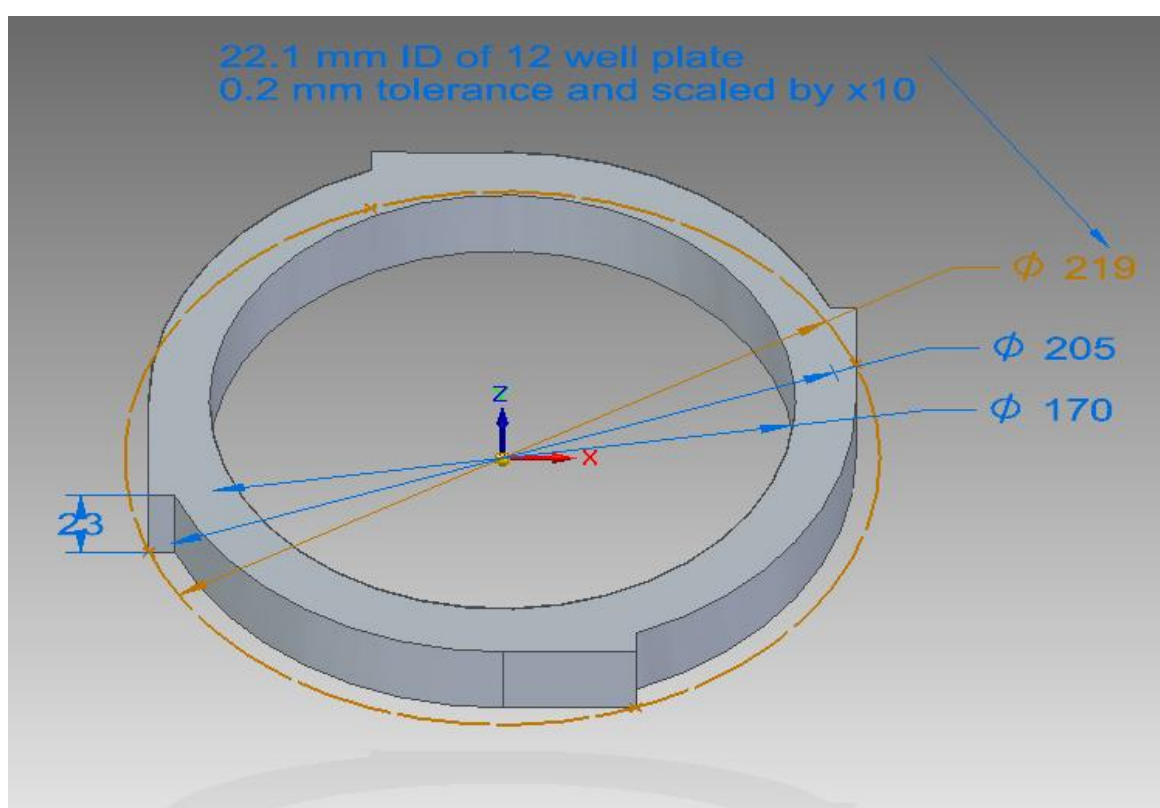


*Figure 3.1* CAD model of a well plate ring that was 3D printed in ABS, used to hold down scaffolds at the bottom of the well plates, note: the measurements are scaled by 10 as a quirk of the STL conversion. The internal diameter of the well plates is 22.1 mm meaning the part must fit within that, hence the 0.2 mm tolerance, 0.1 min clearance and ± 0.1 mm print accuracy. Small centring protrusions were included in the design to maintain a gap at the sides for fluid transport and reduce part diameter reducing print material. The actual print came out too thin to hold all the samples,

due to shrinkage, and were not dense enough to stay on-top of the samples. Future designs should have sprung centring arms at an interference fit with the plates (e.g. 22.1 mm) that will deform exerting pressure against the walls. As well as an internal nesting ring that can support the scaffold and clamp the edges in the outer ring, the inner ring should have enough clearance to compress 20 microns of PLCL scaffold when nested (e.g. clearance of 0.15mm ±0.05).

## 3.5.2 Immunocytochemistry methodology

This technique is not reliable for protein quantification since the brightness of the fluorescence can be altered by changing the gain of the LASER. Thus relative fluorescence cannot reliably be measured across different samples. Instead, the images are a qualitative method of proving there is protein adherence, and if coverage is even.

## 3.6   Method

Prepare samples similarly to the FBS experiment, pristine controls to be submerged in water, one to be submerged in the primary antibody solution and the other not, a negative control for background auto-fluorescence of the PLCL. As well as one pristine and one 500W DBD treated scaffold to adsorb FBS. Wash samples in deionised water to remove weakly bound albumin, and make up 3.92µg/mL solution of primary mouse anti-BSA antibody in molecular grade water. Dropping the solution directly into the middle of the sample to fully submerge the scaffolds and leave for at least forty-five minutes, the longer the antibody has to complex with the albumin the better the result will be.  Wash the samples in deionised water three times and make up a 9.95µg/mL solution of conjugated secondary rabbit anti-mouse immunoglobulin G. Cover all samples, including the negative control, with the secondary antibody solution and leave the solution for no longer than three hours to avoid background fluorescence. Wash the samples once more with deionised water and carefully place the wet scaffold on a microscope slide keeping the sample as flat as possible. Drop excess glycerol onto the scaffold and upturn the slide carefully onto a cover slip, avoiding air bubbles. Seal the edges of the cover slip with clear nail varnish to keep the samples moist. Using a 63x objective lens with immersion oil to take images of the samples with an argon LASER to excite the Alexa Fluor 488nm fluorophore.

# Chapter 4. **Results**

## 4.1    **Electrospun Scaffolds Characterisation**

## 4.1.1 Physical Characterisation

*Scanning Electron Microscopy*

An SEM is used to image the microscopic morphology of the electrospun mesh for statistical analysis of the fiber diameters as well as other features like beading, alignment and fiber thinning that suggest issues with the manufacture of the scaffolds. The manufacturing be able to reproduce viable scaffolds, using a repeatable manufacturing set-up, to ensure the validity of the data and cell response.

Electromagnets accelerate and focus a beam of electrons onto the electrically conductive surface of a sample, the scanning coils raster the electron beam across the sample where the electrons interact with the electrons on the surface of the sample. If the interactions are inelastic, the reflection is called a secondary electron, and if elastic they are backscattered electrons. Characteristic, continuum and fluorescent X-rays are produced microns inside the material, which are useful for elemental analysis using the SEM. A characteristic x-ray is emitted by an electron that fills the inner shell valence from a secondary electron collision and continuum x-rays are when electron accelerates or decelerates. X-rays are generated at high beam voltage for elemental analysis, but since the PLCL scaffolds are complex, the elemental make-up of the sample is not useful for characterisation.

Using a low accelerating voltage (below 5keV) results in a higher yield of backscatter meaning improved surface resolution making for better conditions to image the topography of the fibers, as well as allowing higher magnification (Pretorius 2009).

To analyse the samples x2500 and x1000 SEM images are converted to black and white by ImageJ and the DiameterJ plug-in, and the resulting segments are compared with the original image to remove artefacts created by the software; be sure to save the "processed" images as 8-bit greyscale '.TIF' files. x2500 magnification images are chosen because the fibers are large enough for manual processing using Photoshop CS6. However, there are fewer fibers for DiameterJ to analyse, this is not significant if more than three files are analysed from each sample. The data is stored as Comma Separated Values (.csv) files and can be read into MatLab R2018a (MathWorks, Natick U.S.) to produce radius or diameter histograms.

Comparison of 9:1 and 8:2 Chloroform to DMF

The chemical composition of the PLCL will not be affected, but due to the differing volatility, porosity may be affected which would affect the surface area. Graph 1 suggests that the fibers are thinner when deposited on a rotating mandrel with an average diameter of 0.861 µm with a standard deviation (σ) of 0.237, whereas the 9:1 solution deposited on a stationary collector had an average fiber diameter of 1.169 µm and σ = 0.451. Using samples with a smaller diameter will more closely replicate the components of the ECM, as well as the more narrow range, 8:2 solution spun onto a mandrel appears the most applicable method of scaffold production.
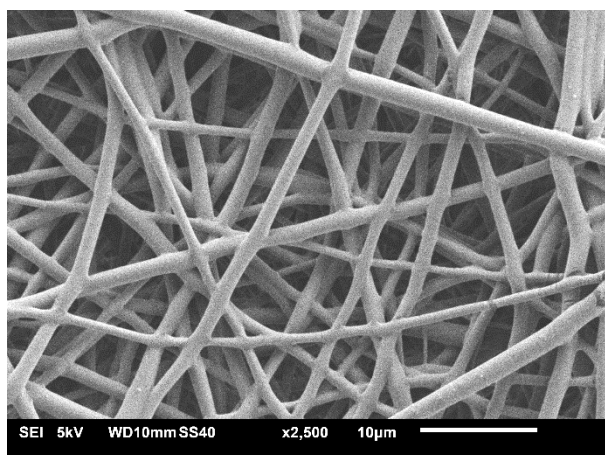
*Figure 4.2* SEM 9:1 CHCl3 : DMF, spun onto stationary collector. Fibers appear to melt at some junctions, fusing the fibers together.
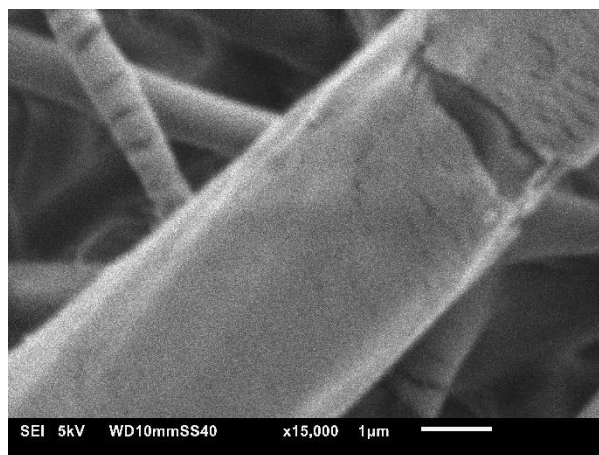


*Figure 4.2* SEM 9:1 solution, x15,000. A mild repeating wave pattern on the surface, some cracks due to air exposure or stress, may be an accelerant to degradation.
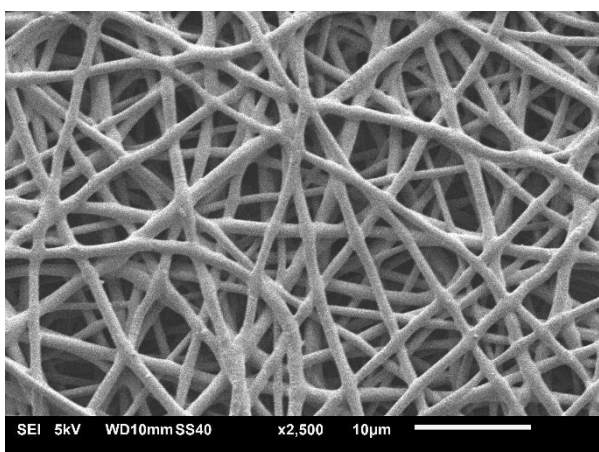


*Figure 4.3* SEM 8:2 solution, stationary collector. Fibres meld together at junctions and droop slightly between the support of other fibers.
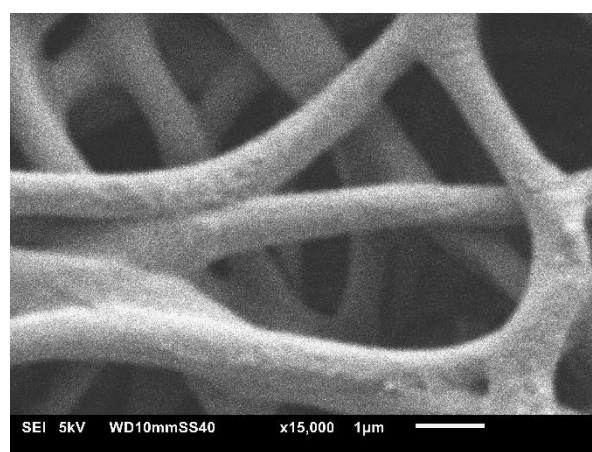


*Figure 4.4* SEM 8:2, x15,000. Interesting nano-topography, rippling on the internal diameter of curved fibers, suggesting the bend occurred after the solvent evaporated.
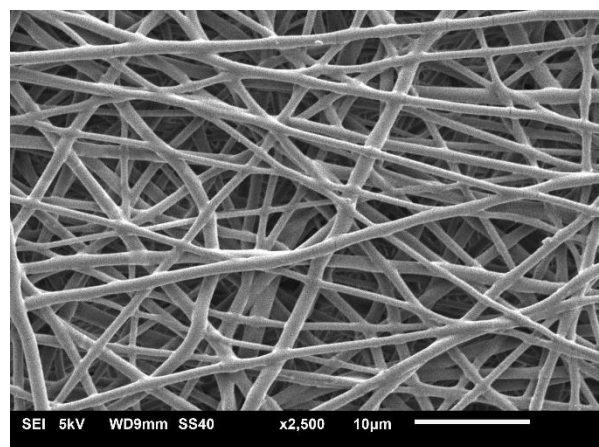


*Figure 4.5* 8:2 solution, rotating mandrel. Fibers have no obvious alignment as a result of the rotation, with some evidence of meld.
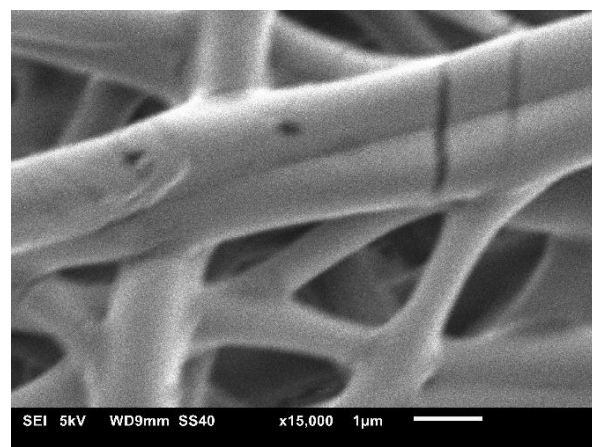


*Figure 4.6* Less topography than 4.4 and 4.2, and also shows damage to the fiber, not the gold coat or else there would be electron charging not more shadow.

The static 8:2 solution appears to create the most topography as seen in fig 4.4, the ridges and bumps would make good anchor points for cell integrins when functionalised. And as seen in the figure 4.2, stationary collectors seem to create more topographical features than the rotating mandrel, but for simplicity of the experiment, smooth fibers will make an adequate stating point.

**Graph 1** Histogram of fiber diameters of different solution ratios for Chloroform (CHCl2) : DMF and on different collectors. Mandrel spun 8:2 CHCl2 : DMF scaffolds have the tightest distribution and the smallest average radius. Thinner fibers are closer to the diameter of ECM components like collagen, and so may better predict cell response.
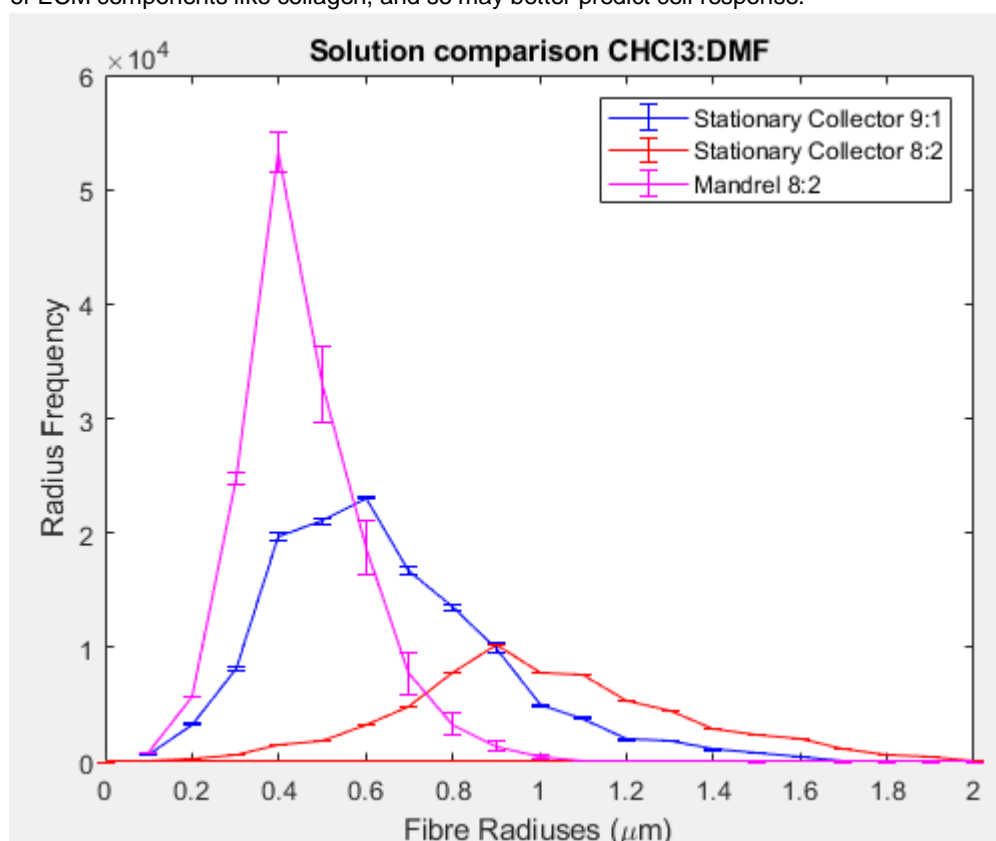


**Table 1** The average pore area and fiber diameters of the different solutions and collector geometry spun at 15 cm, stationary collectors use a flow rate of 1 mL/hr and the mandrel was set to 2 mL/hr. Mandrel samples have a more consistent fiber diameters that the stationary collectors.

| | Average Pore Area ($\mu m^2$) | Pore Standard Deviation, σ | Average Fiber Diameter (μm) | Fiber Diameter σ |
|---|---|---|---|---|
| 9:1 Stationary | 7.049 | 14.013 | 1.169 | 0.451 |

| 8:2 Stationary | 9.600 | 15.968 | 1.944 | 0.578 |
| 8:2 Mandrel | 4.431 | 6.596 | 0.861 | 0.237 |

Graph 1 and table 1 summarise the difference between the resulting scaffolds from stationary and rotating collectors, in efforts of optimising and problem solving production. Mandrel scaffolds required less supervision, replace the tin foil begin spinning and occasionally wipe the tip as the Taylor cone slowly destabilises over five to ten minutes and begins multi-jet spray, this would go on for an hour. Where-as the stationary collector plates took ten minutes to spin 20 micron thick samples, the cone would destabilise every 1-10 µL deposited. This meant these samples had to be carefully watched to avoid dripping, or the voltage reduced, increasing the size of fibers (Varesano, 2015) making the fibers even less analogous to ECM components.
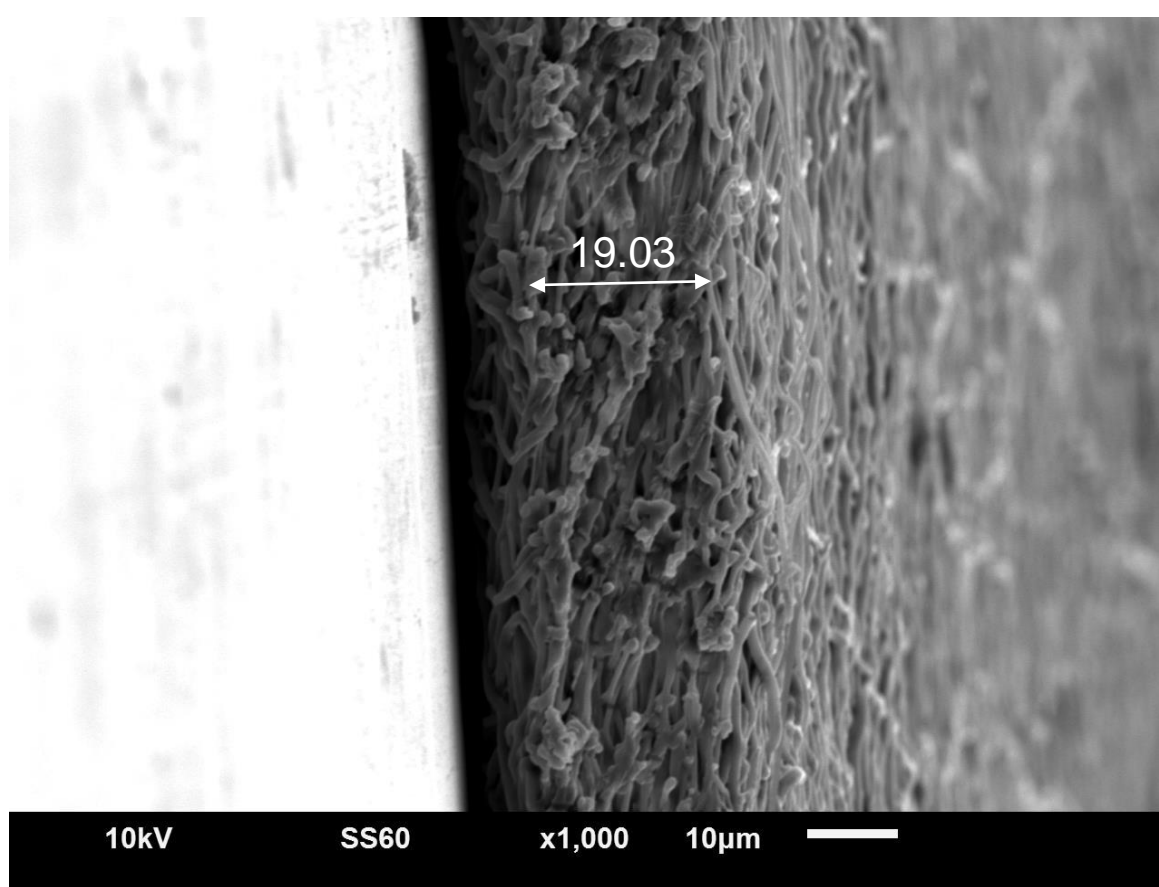


*Figure 4.7Results.* SEM of a mandrel spun 8:2 solution scaffold thickness after 1 hour of 2mL/hr. The thickness of the control scaffolds are 19.03 µm ±1.01, thickness appears even. A section across the sample shows the non-discrete layering in the polymer.

As seen in fig 4.7, samples are spun to a thickness of around 20 microns, this is to give them structural support and mass to resist floating in the cell culture media (Mahmoudifard *et al.*, 2016). Imaging cross sections was achieved by cutting a strip of material with a sharp razor or scalpel and mounting vertically in the SEM machine, samples were checked for thickness

before DBD treatment and peptide submersion. The pores and gaps between the fibers extend through the thickness of the material explaining why electrospun polymers are used for membrane filtration, the many layers are tightly packed and can be further densified by increasing the spinning distance, elongating the fiber.

## 4.1.2 Chemical Characterisation of scaffolds

*Fourier Transform IR Spectroscopy*

Take a spectrum reading of the air to be removed as a background, meaning the atmospheric conditions will not be a variable when imaging the samples on different days.

**Graph 2** Control PLCL ATR-FTIR analysis, absorption spectrum. Peaks are consistent with analysis of PLCL, however 2362.39 cm$^{-1}$ peak may be contamination, possible contaminants that would fit in this region includes water..
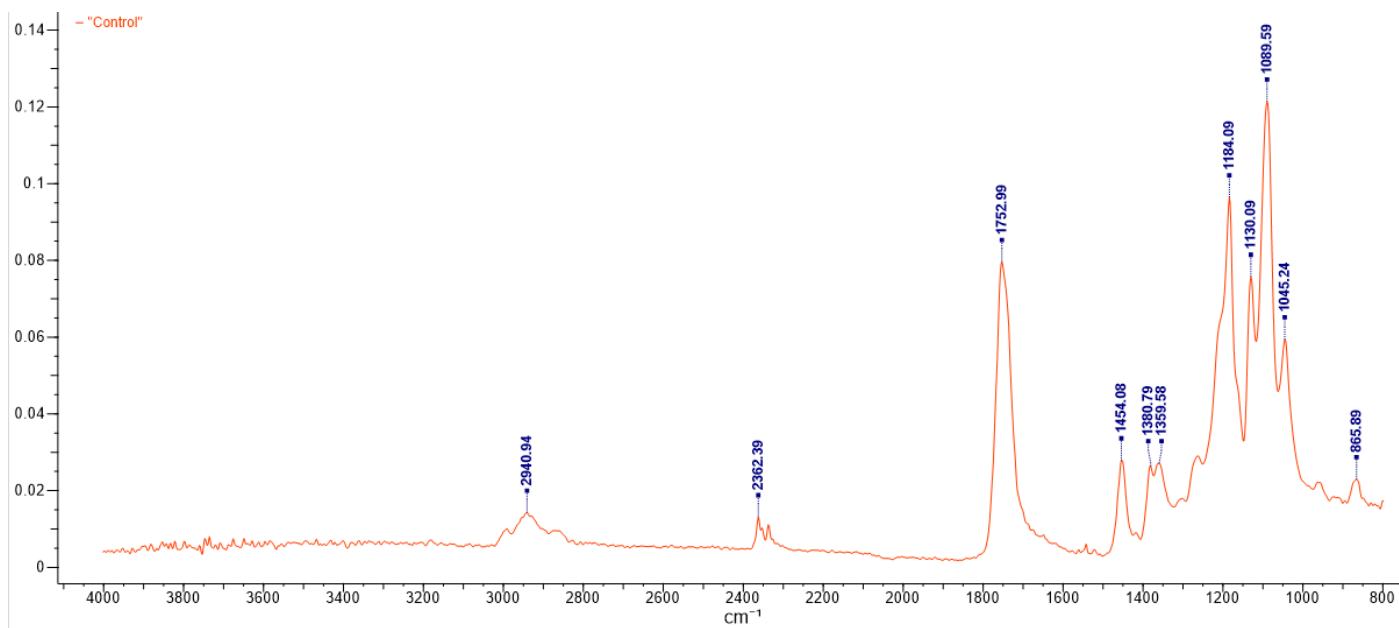


Comparing this sample to the Sigma Aldrich FTIR chart, there is evidence of an ester bonds in an organic polymer: the broad weak peak at 2940cm$^{-1}$ could be intramolecular O-H stretching in an alcohol or carboxylic acid group, though the carboxyl group is normally stronger and centred around 3000cm$^{-1}$, or C-H stretching in an alkane would exhibit a medium broad between 3000 and 2840. The weak peak at 2362cm$^{-1}$ doesn't correspond with any expected chemical groups, though it could be a result of small amounts of O=C=O stretching that normally exhibits a sharp peak at 2349. Strong peaks around 1753cm$^{-1}$ are common in C=O containing compounds, so this could be carboxyl acid (1760), esters and δ-lactones (1750-1735) which is pretty telling since the polymer measured is a polyester of lactide and caprolactone that will have carboxyl acids at the un-polymerised chain ends. In the fingerprint

region after 1500cm$^{-1}$, bond peaks are more specific to the chemical. 1454 medium peaks are C-H bending probably indicating the presence of methyl in alkanes. 1380.79 cm$^{-1}$ medium peaks could be C-H bending in aldehydes (1390-1380) or gem dimethyl (two methyl groups on one carbon atom at 1385-1380) or O-H bending in alcohol groups (1420 and 1330) or in phenols (1390-1310), with such a broad region the multi-peak could be explained but none of the compounds exhibit any oxygen single bonded to a hydrogen, this could be a result of absorbed water molecules. 1210 – 1163 strong peaks indicate the presence of C-O ester bond stretching, corresponding to the 1184cm$^{-1}$ peak. The peak at 1130cm$^{-1}$ is difficult to place since there are many competing groups that could be placed here, like C-O stretching of an aliphatic ether (1150-1085), tertiary or secondary alcohol (1205- 1124 or 1124-1087). 1089.59cm$^{-1}$ could be a result of C-O stretching of primary alcohol groups on the un-polymerised chain ends but considering the height of the peak there is more absorbance than would be expected from this source. It could be a result of multiple different ether groups along the chain absorbing slightly different wavelengths due to the bonds atomic environment. The medium/weak peak at 1045 is more likely to be environmentally altered primary alcohol groups, it is unlikely to be S=O stretching (1070-1030) since these are normally strong peaks, and no other strong peaks coincide with any expected sulphur peaks. It could be a strong broad peak of a CO-O-CO anhydride that may have a minimal presence due to the isomer of the polymer chain is less common than the ester bonding which remains in the range of ether groups. These peaks are consistent with FTIR analysis by Song *et al.* (2016) for PLCL.

Chloroform would be represented by a strong peak between 850-550 cm$^{-1}$ indicating Cl-C bending, which is not visible, and the weak peak at 865 is not evidence of residual CHCl$_3$.

DMF would exhibit a medium C-N amine peak stretching between 1250-1020cm$^{-1}$ and 1450cm$^{-1}$ C-H methyl group peaks and a strong primary amide C=O bond 1690cm$^{-1}$. Other than the difficult region between 1200 and 1040cm$^{-1}$ there is little evidence that there is residual DMF remaining.

## 4.2   Plasma Treatment
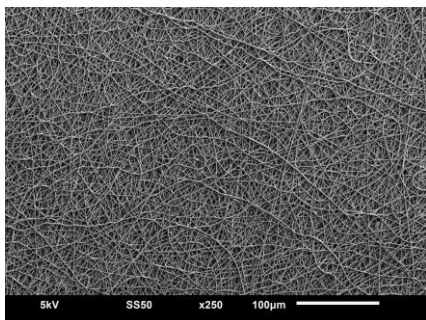
## 4.2.1 Physical Characterisation

SEM

***Figure 4.8*** Control sample 8:2 mandrel spun. Random fibres within normal range
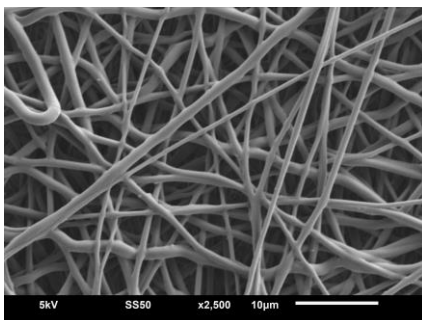


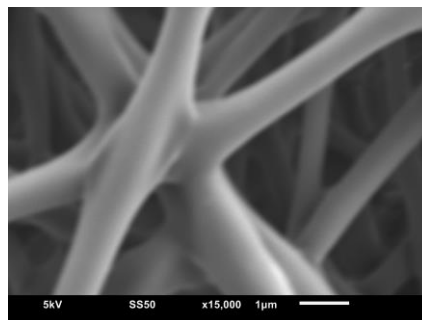***Figure 4.9*** Control x2500. Some dust contamination, but smooth, intact and lightly fused fibers



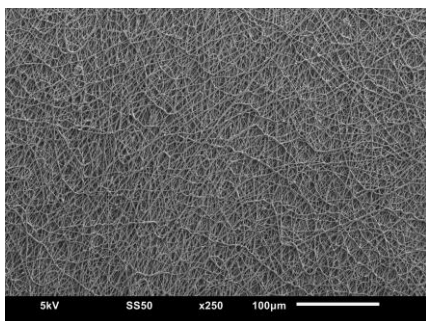***Figure 4.10*** Control x15000. Joints have fused during spinning, minimal topography.



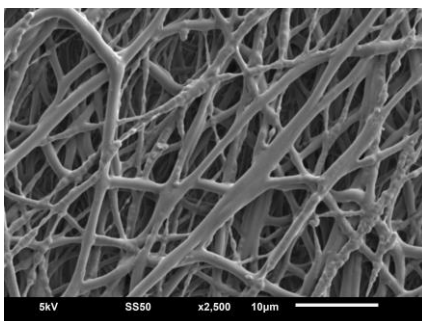***Figure 4.11*** 250W DBD treated 8:2 scaffolds. Fiber network is intact.



***Figure 4.12*** 250W x2500. Some fibre melt and bubble formations in thinner fibers.
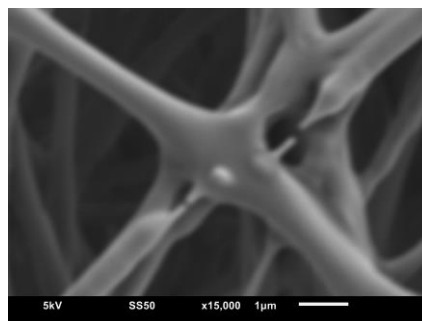


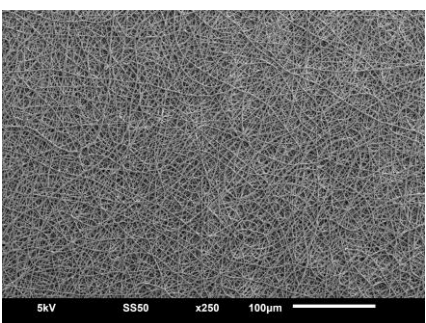***Figure 4.13*** 250W x15000. Rippling texture across the surface, still smooth compared to ECM. Fiber elongation.



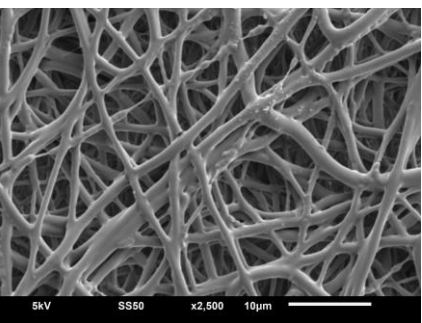***Figure 4.14*** 500W DBD treated samples. Network beginning to weaken.



***Figure 4.15*** 500W x2500. Stretched fibers are still connected, meaning structural integrity may remain.
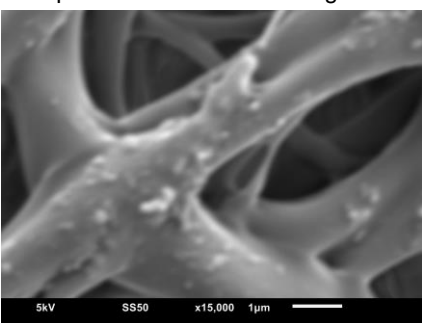


***Figure 4.16*** 500W x15000. Rough topography on many fibers is preferable for cell motility.
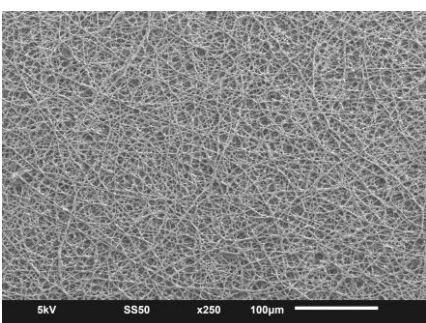


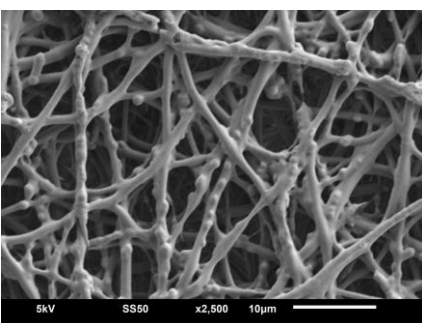***Figure 4.17*** 750W DBD treated samples. Network disconnection.



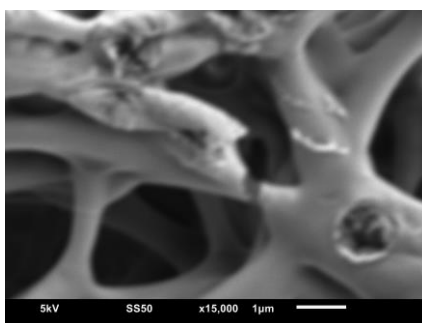***Figure 4.18*** 750W x2500. Fibers thicken as others melt and meld together.



***Figure 4.19*** 750W x15000. Excess chain scission and thermal damage results in interesting topography.
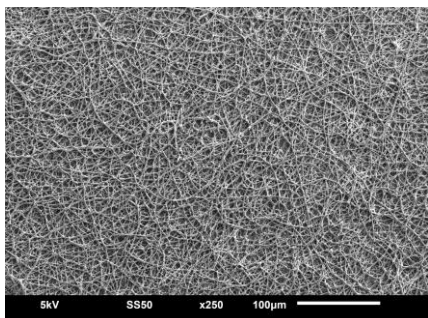
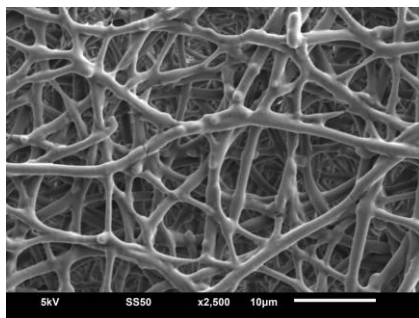***Figure 4.20*** 1000W DBD treatment. Network damage and increased pore sizes.



***Figure 4.21*** 1000W x2500. Thick fibers, with reduced interconnections and large knobbed formations.
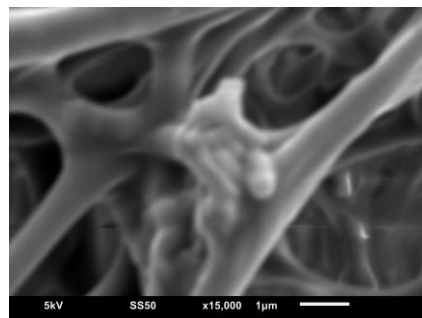


***Figure 4.22*** 1000W x 15000. Thin fibers have completely melted and junctions have rounded, fibers have smooth topography again.

Natural polymers and those found in the ECM tend to be very topographically interesting, collagen fibres have corrugations across their diameter. Cells respond to a surface depending on its topography, governing cell shape or attachment points for the focal complexes and adhesions (Biggs *et al.*, 2009). 250 watts (fig 4.13) is not sufficient to create much texture on the surface of the fibers, and graph 4 shows that the contact angle of 250W is still higher than that of 500W. This power level does create topography, but the nano-topography of 500W is a preferable result.

Any treatment of DBD plasma causes damage to the fibres, and until 500W, the damage to the fibers was insufficient to melt them to the point of breakage. This suggests that 500W is the most applicable with good topography and intact fibers, some structural damage is acceptable since the copolymer's composition can be modified to achieve the desired mechanical characteristics. The damage to the 750W scaffolds like fig 4.19 shows fibers have physically separated weakening the material, and fig 4.22 shows when the heat is too much, said separated fibres amass leaving shadows of the former network.

**Graph 3** Fiber radius histogram, measuring variation across different treatment powers of DBD plasma were applied to the scaffolds. With a minimum of 5 pictures of each sample yielding at least thousands of radius measurements each. Error bars represent variation of distribution rather than measurement variation, the data is grouped in discrete radiuses by the software resulting in some statistically acceptable error.
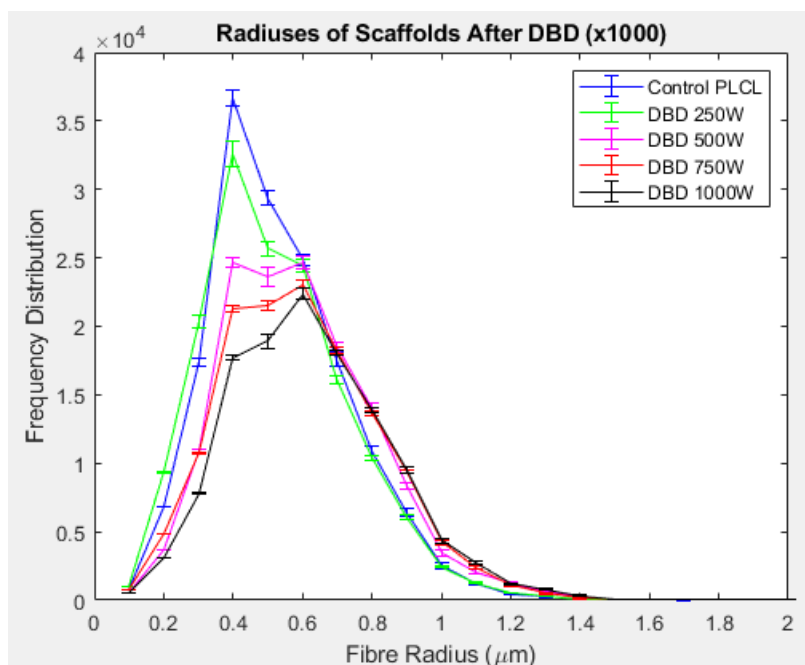


**Table 2** Average pore areas and fiber diameters of scaffolds after DBD power treatment. ImageJ pore data is unreliable since the SEM images are only 2-dimensional representations, pores in electrospun polymers are 3-dimensional and so the depth of the pore and the interconnectivity cannot be determined.

| Sample | Average Pore Area ($\mu m^2$) | Pore Standard Deviation ($\sigma$) | Average Diameter ($\mu m$) | Diameter SD ($\sigma$) |
|---|---|---|---|---|
| Control | 5.031 | 7.428 | 0.985 | 0.372 |
| 250W | 6.973 | 10.472 | 0.969 | 0.400 |
| 500W | 4.767 | 7.027 | 1.113 | 0.421 |
| 750W | 4.108 | 7.494 | 1.138 | 0.450 |
| 1000W | 8.266 | 15.846 | 1.192 | 0.445 |

The average pore sizes of the DBD treated scaffolds compared to the control don't suggest any particular pattern, any variation can therefore be attributed to the random deposition of the fibres and the limitations of the imageJ software.

The diameters of control and 250W fibers seem to indicate thinning, but the variation across the table is within the standard deviation of the electrosping set-up. However, since the experiment was performed on the same sheet of electrospun PLCL, the original fiber diameters should not vary by much in distribution, so the trend of the table towards fiber thickening is not unreasonable. Graph 3 shows a slight shift to the right for all the samples after 250W of plasma, the fall in peak height suggests there are fewer fiber sections for imageJ to measure. This could be as a result of the fibres melting, disjoining and leaving a space where the software will not measure. This is supported by the slight change in thickness, since damaged polymer mass would likely recoil into the remaining fiber leaving a thicker bulb as seen in figs 4.17 and 4.20.

**Graph 4** Contact Angle Comparison of Different DBD Power Treatments. The graph clearly shows a trend that DBD treating the samples decreases the contact angle by at least $20^{\circ}$
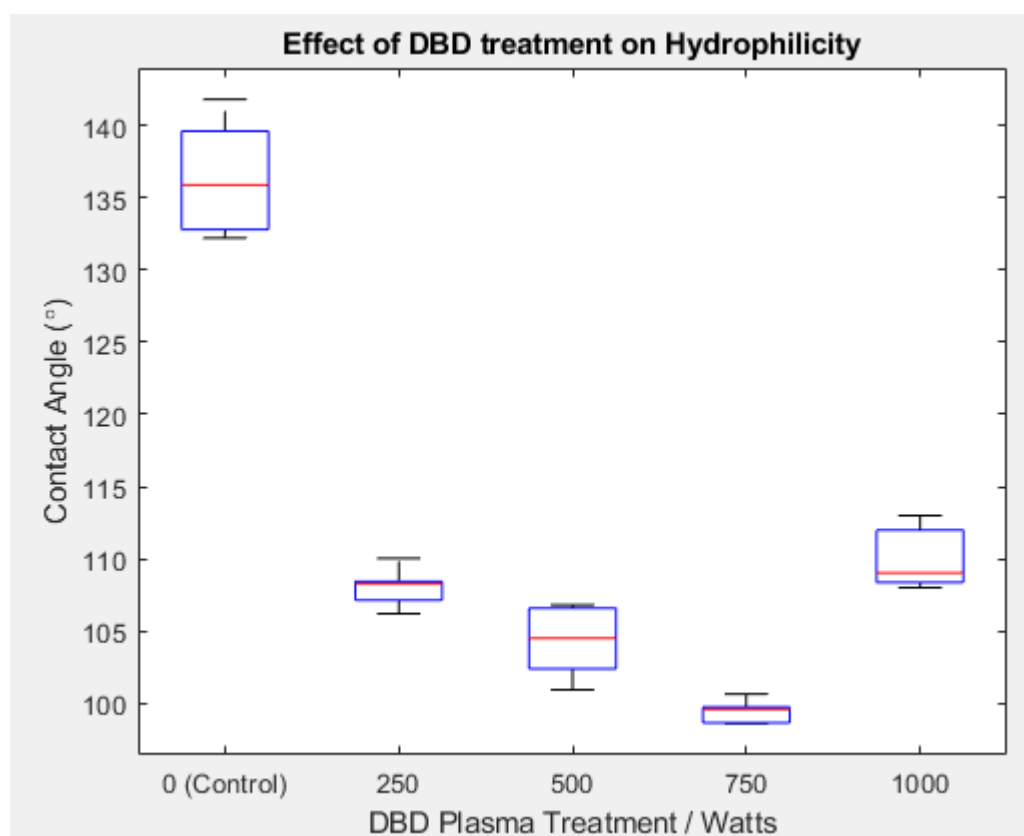


DBD treated samples are more hydrophilic than the control sample, however as seen in graph 4 at 1000W, the contact angle begins to increase. This parabolic trend suggests that the treatment of a surface by cold plasma can be used to decrease and increase hydrophilicity (Xu *et al.*, 2013). 750W has the lowest contact angle measurement dropping by $35^{\circ}$, but as seen in figs 4.17 and 4.18 the fibres themselves are too badly damaged, forming undulating fibers where they have thinned repeatedly and create what look like strings of beads. 500W has

improved hydrophilicity of 30º with some variation across the measurement, likely due to human error or surface variation.

## 4.2.2 Chemical Characterisation

**Graph 5** The FTIR analysis of DBD treated PLCL (top) and a control sample of untreated PLCL (bottom)**,** the scale of the graphs cannot be set separately, thus the control sample is small. This is a cosmetic detail, when inspected against for peak position, the samples are similar enough to suggest little to no change.
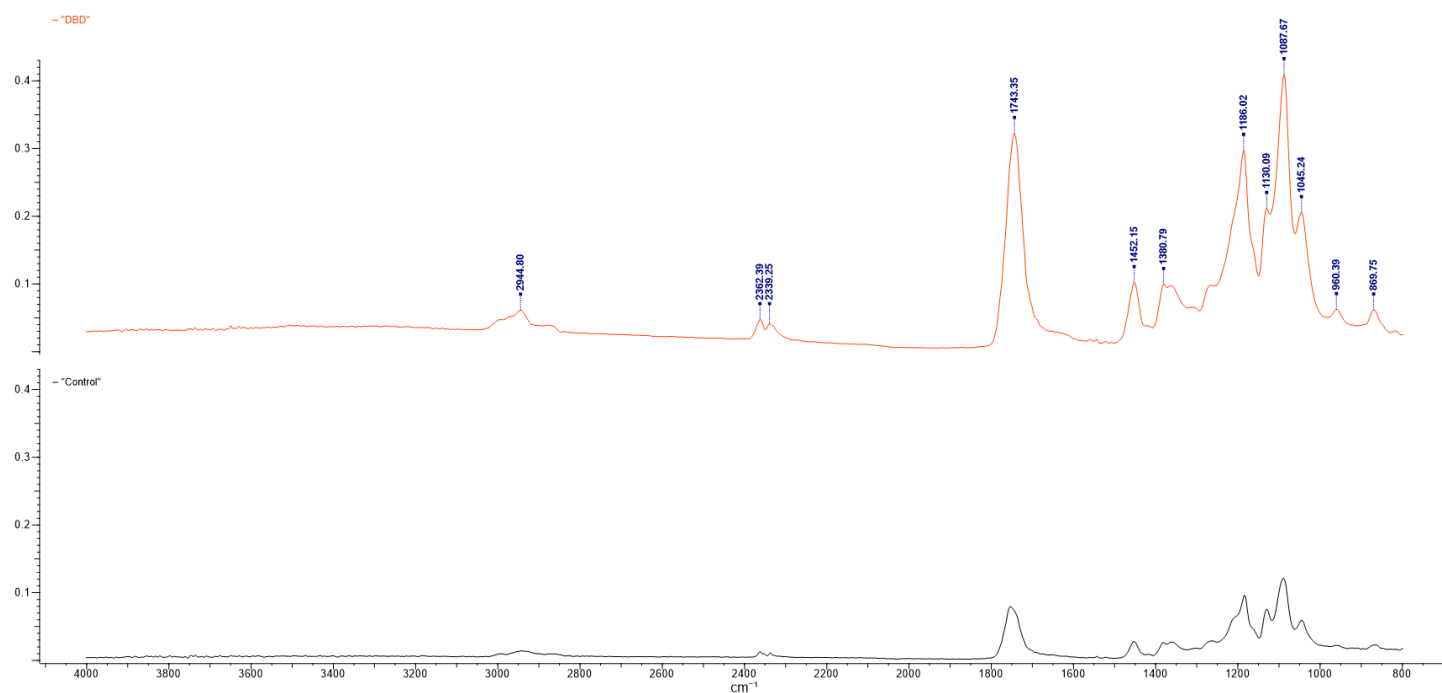


*FTIR*

There is little change to the peaks positioning and relative peak height compared to the control PLCL scaffold, however the scale of absorption has changed. Since the positions of the peaks have remained in the same place, it can be concluded that there is little to no chemical change to the PLCL molecules after DBD treatment. (Smith 2015) Peak height is affected by concentration measured, as seen in Graph 2, the peaks of DBD treated PLCL have similar shapes so the bonds measured are most likely the same.

## 4.3    Protein Adsorption

Due to poor experimental conditions dust particles were able to settle on the samples, this may be due to excessive handling trying to keep the samples flat to the microscope slides. An alternative source of particle contamination could be the down flow of air from the H14 HEPA filter in the class 2 biohood. Since HEPA filters have an efficiency of 99.97% for 0.3 micron particles, since these particles measure between 0.28 and 0.78 μm it is unlikely this is a

contributor. Sample handling is the most likely source of dust particles since there is variation between samples after taking more care in handling the samples.

## 4.3.1 Physical Characterisation

SEM images of the samples reveal dust particles adhered to the surface of the control fibers as well as the other samples, with more care taken to avoid contact with dust there were fewer particles on the samples.
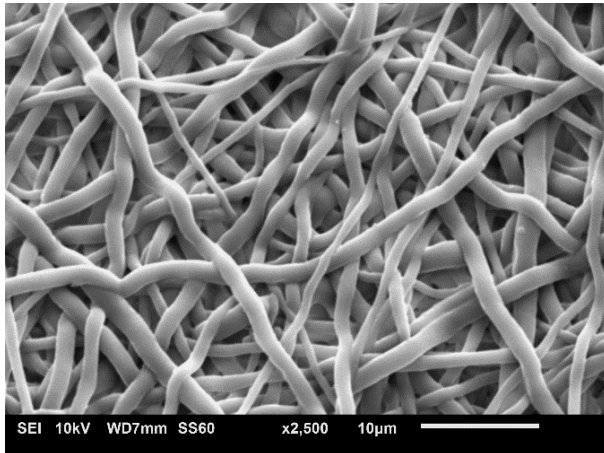


***Figure 4.23*** SEM Control scaffolds. Samples appear to have less space between fibres.
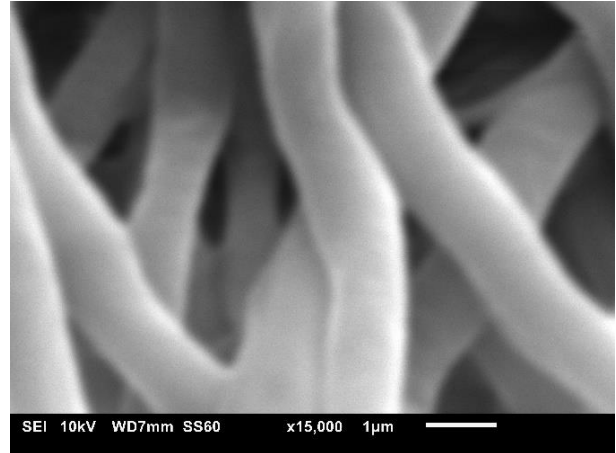


***Figure 4.24*** Control scaffolds x15000. No apparent change to topography due to water.
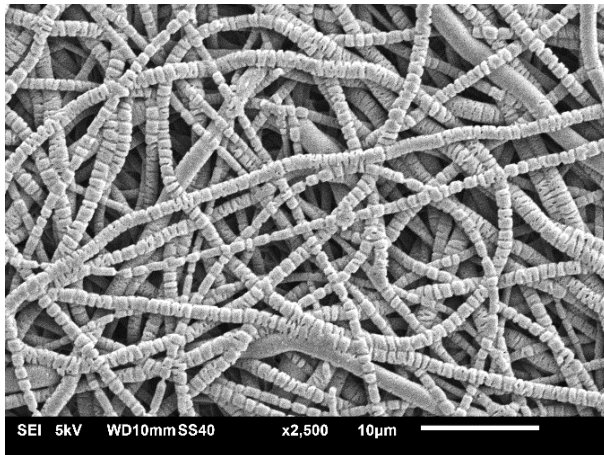


***Figure 4.25*** Pristine PLCL with FBS. Bands of damage appears to be roughly 100 nm or so deep
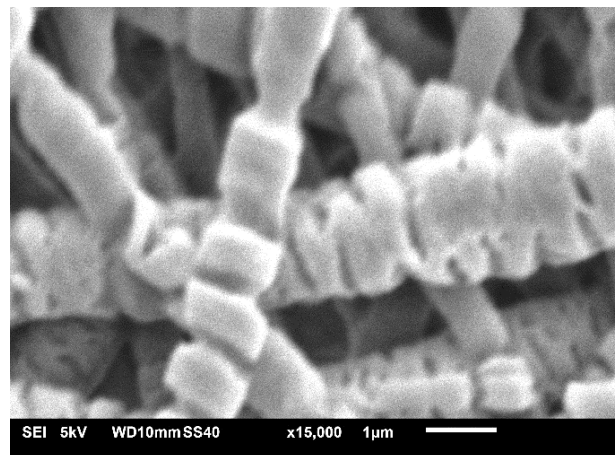


***Figure 4.26*** PLCL + FBS x15000. Increased surface area and likely reduced mechanical strength.
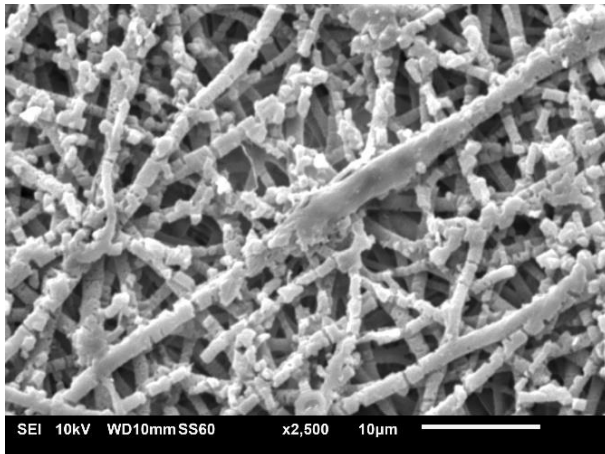
**Figure 4.27** 500W DBD treated PLCL with FBS. Total erosion through the diameter of some fibers and pitting of the surface.
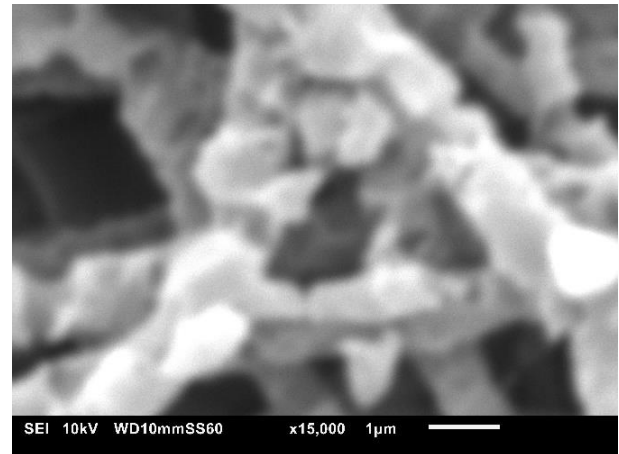


**Figure 4.28** DBD and FBS x15000. Barely recognisable fibers due to excess damage. Shaddows of the main fiber structure appear through cracks in a surface layer
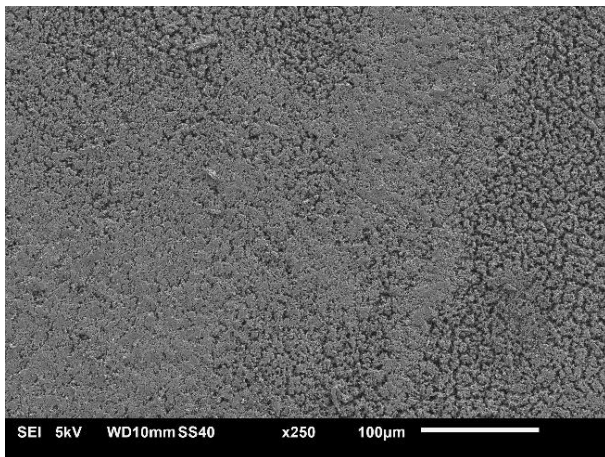


**Figure 4.29** 500W DBD and FBS treated sample x250. Does not show characteristic fibres of electrospun polymers.
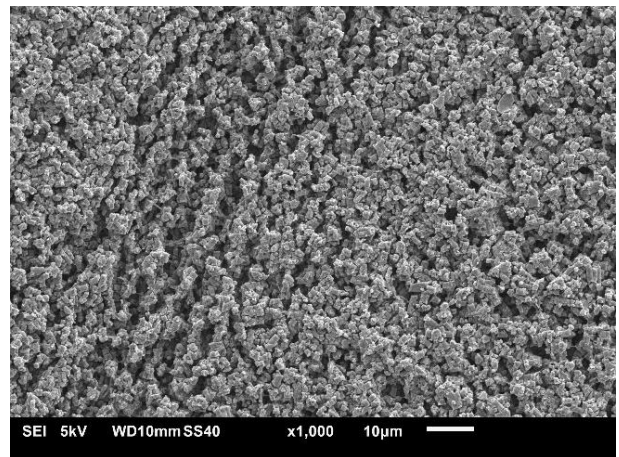


**Figure 4.30** DBD and FBS x1000. Fissure like formations in the blanket of irregularity, could indicate tension forces.
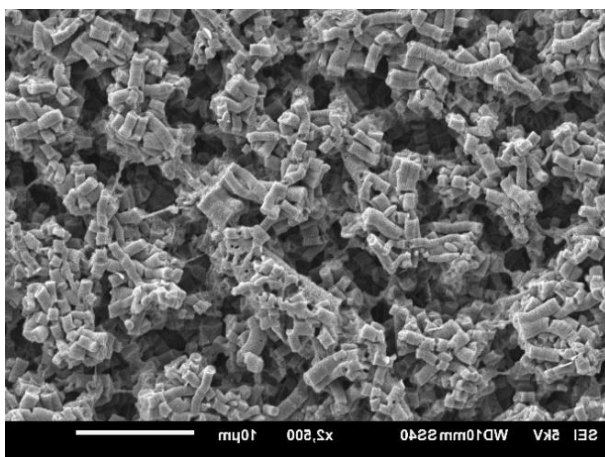


**Figure 4.31** DBD + FBS x2500. Deep channels of broken fibers that no longer interconnect.
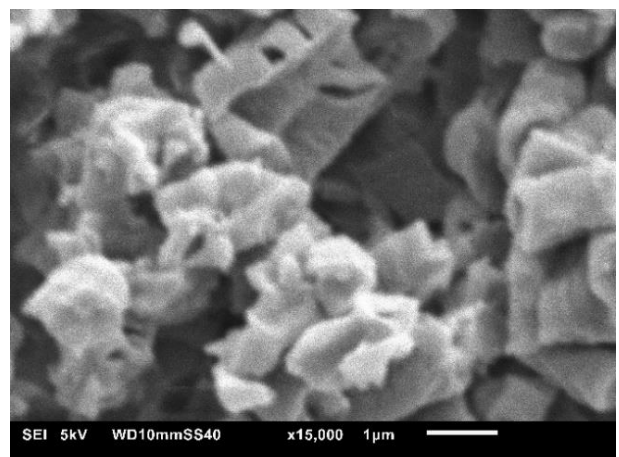


**Figure 4.32** DBD + FBS x15000. Unrecognisable chunks of fibers that have broken apart.

Figures 4.29-32 has excessive change to the fiber morphology, this scaffold had to be teased from the well plate. This is damage that could have been caused by the samples adhering to the surface, causing stresses to be applied unevenly in the material when moved. This amount of damage to the sample suggests a major human error in experimental conditions. Damage seems to be inevitable since it is a biodegradable polymer, the mechanical strength will degrade as the chains are hydrolysed, and thus the extent of the damage in vivo conditions must be established.

Gao *et al.* (2018) discus the degradation of poly(ε-caprolactone) (PCL) over 150 days in phosphate buffered saline and how degradation  is affected by changing proportions of poly(lactic-co-glycolic acid) (PLGA). The degradation of (fig 25-26) looks most like the enzymatic degradation of Gao *et al.*'s 90/10 PCL/PLGA scaffolds. Still the unresolved factor is the incredibly short time period of the damage. The increased damage in figure 4.27 and 4.28 could be a result of the reduced contact angle increasing hydrolytic interactions, and as the polymer is degraded the pH will be reduced by the acidic metabolites catalysing the hydrolysis. This however, does nothing to explain the degradation of native PLCL in heat inactivated FBS, since scaffolds are left in culture media over 24 hours for cell culture.

**Graph 6** Fiber radius distribution of the scaffolds after FBS experiment, since BSA is 6.74 nm there should not be any statistical change to the fiber dimensions.
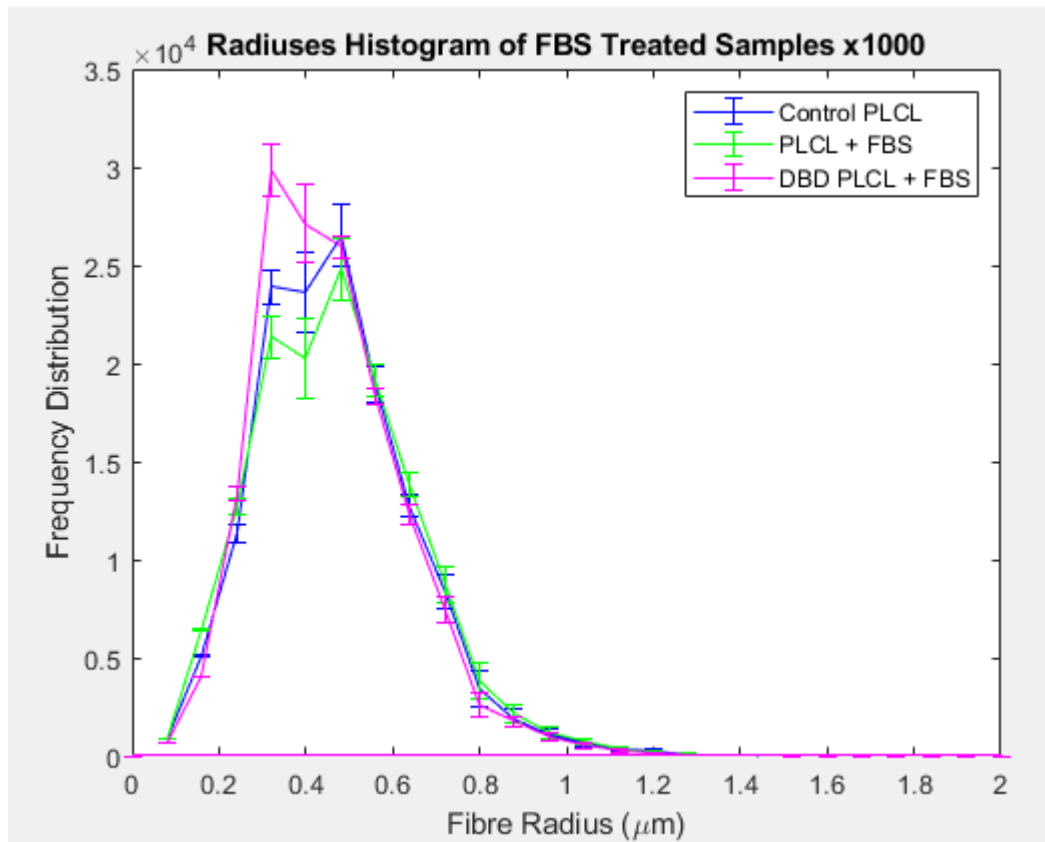


Average pore area of the control samples are 2.920 $\mu m^2$ with a standard deviation of σ = 6.664, pristine PLCL + FBS: 2.132$\mu$m σ = 4.748; 500W DBD + FBS 2.620$\mu$m σ = 3.701 which is significantly smaller than the average pore sizes of the unwashed 8:2 control (5.031$\mu m^2$) and DBD treated samples (4.767 $\mu m^2$), that have a pore area range between 4.108 to 8.266 $\mu m^2$.Because the FBS trial sample pore areas are so much smaller than the production samples with a decreased standard deviation, the reduction is likely due to shrinkage of the fiber mesh.

Contact angle measurements failed due to the PLCL scaffolds not remaining flat to the slides during measurement, thus the optical device was hindered. This could be fixed using a different method of holding the samples, during the FBS trial, the scaffolds escaped from beneath the rings and could float to the surface requiring intervention, meaning more opportunities for contamination and damage to the PLCL fibers. If the material is suspended under tension around a ring like a drum skin, the taut surface would be relatively flat and an attached ring would be easier to position. This method would require more sample preparation

Damage to recent samples is not consistent with the first experiment, but as explained by Augustine *et al.* (2015) PCL (Mw =70,000) can degrade hydrolytically in water over 30 days, especially if the polymer has been made more hydrophilic by plasma treatment or the adsorption of proteins like those found in FBS or simulated body fluid. However, the samples are not from a 30-day degradation study, but a 24-hour FBS adsorption, when compared to the samples that were soaked in water only; the FBS treated PLCL exhibited much more damage to fibers and striations of degradation across the fiber diameters even though it is water that hydrolyses ester bonds. Since the damage doesn't appear to be in one direction, excess torsion does not appear to be the main cause but aided by the reduced mechanical stability of the material after adsorption. The higher molecular weight of the PLCL used in this experiment (202,000 g/mol) should make these fibers more resistant to changing mechanical strength in such a short time because there are more ester bonds to break. As well as larger spherulites increasing the surface area to volume ratio of the crystallised region of the polymer, but more amorphous intergranular space that is susceptible to degradation.

When removing from the surface of the well plates some samples adhered better than others and so would have required more force to dislodge them. This increased adherence was more noticeable for the FBS treated samples, possibly due to the mass of the adsorbed protein increasing the density of the polymer, so they don't float during washing and remained flat to the well plate. Improving experimental conditions would require a ring that can maintain pressure against the plate walls keeping the samples at a set height from the bottom, but not touching it, more likely suspending the scaffold in a secondary inner ring. The issues with this include; an overly tight fit may not allow the solution to fully surround the fibers. This may weigh down the middle of the sample, stretching the interchain forces sagging the material so it sits, wrinkled on microscope slides for contact angle measurement.

Flat and clean samples are essential for getting a reliable measurement of contact angle, see fig 5.1, and so flatten them between 2 glass microscope slides and pressing them with a large book overnight. The scaffolds that had slight cupping before pressing, formed expanding ripples that changed the angle measured by the software and physically obscures the camera making imaging inaccurate.

## 4.3.2 Chemical Characterisation

**Graph 7** FTIR spectra of DBD treated (top) and pristine PLCL (middle) soaked in FBS and the control sample (bottom).
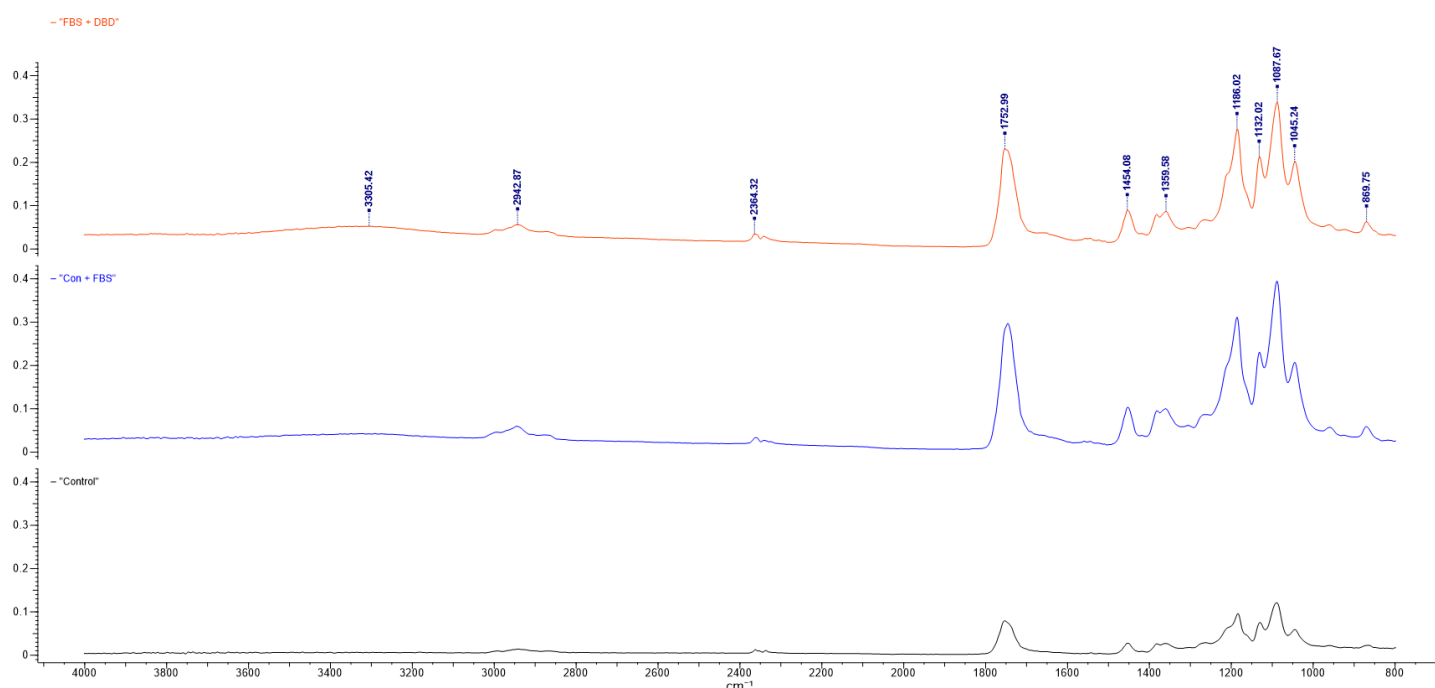


On the FTIR spectrums of the FBS treated samples an additional broad peak is discovered at 3305, and the DBD treated sample appears to have a greater peak than that of the pristine PLCL fibers. This peak could be a result of a range of different molecules; O-H stretching alcohol (3550-3200) would have a larger peak. 3500 and $3400cm^{-1}$ medium peaks could suggest the presence of N-H stretching in primary amines or between 3400 and 3300 as well as 3330-3250 stretching in primary aliphatic primary amines. But since FBS is a complex mixture of proteins and hormones the very broad peak could be from the many amine groups. All with slightly changing atomic environments spreading the waveform across a wider range. Since the peak is so short, this could be a statistical anomaly, or evidence there is a minimal concentration of peptides bonds.

*Immuno Cyto Chemistry*
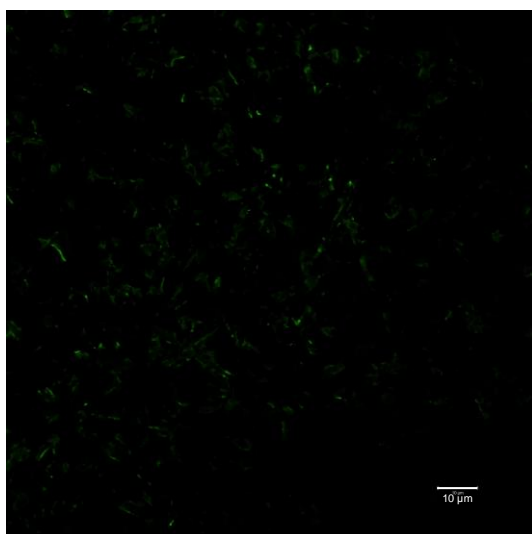


**Figure 4.33** Confocal negative control, submerged in water, no primary antibody. Any fluorescence is a result of auto-fluorescence or trace amounts of Alexfluor trapped between the fibers, no fibers are visible.
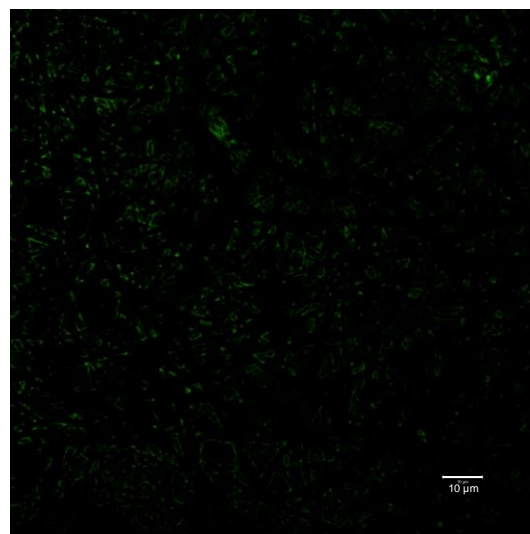


**Figure 4.34** Confocal control PLCL fibers, submerged in water. This image appears like a negative image of the fibers, the BSA specific primary antibody did not bind to the fibers thus the pore spaces may be filled with the fluorophore.



**Figure 4.35** Confocal image of BSA adhered to a pristine PLCL fibers. Barely visible fibers meaning antibodies have bound to the fibers, but there may be too few fibers in the focal plane to see much fluorescence. Image was taken using the same LASER settings as 4.35.
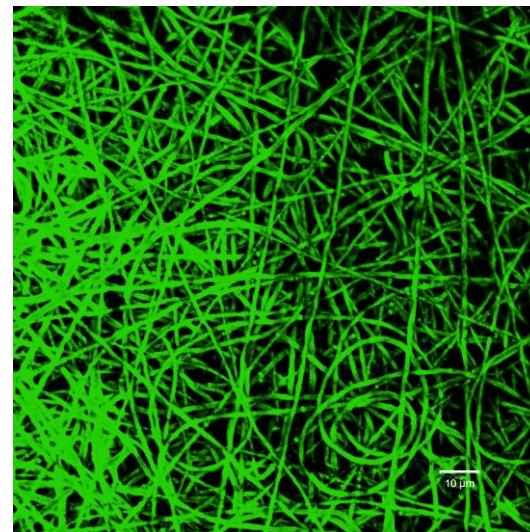


**Figure 4.36** Confocal image of BSA adhered to a DBD treated PLCL. Strong fluorescence in areas (left) is a result of fibers being closer to the focal plane of the microscope, but points along the fibers are topographical features where there is more surface for BSA to bind to.

The negative control in fig 4.32 shows minimal auto-fluorescence of the PLCL samples, as the fibers are not clearly visible. The sample does not look electrospun, which would be expected if it was the PLCL that is fluorescing and not the Alexafluor, the porous structure may have trapped the fluorophore during the wash steps. Fig 4.33 is the control sample that appears to have a more fibrous structure than the primary negative control, although, none of the fibers are visible meaning more Alexaflour is present, but none is bound to the surface. Imaging of the pristine PLCL that was coated in FBS, fig 4.34, was found using a higher LASER gain and then reduced to match that of figure 4.35. Individual fibers are barely visible, this means bovine serum albumin does bind to PLCL. The brightness of the fibers may be a result of the focal plane not being in line with many surface fibers. DBD treated PLCL fibers have shown up as bright green fibers, meaning the albumin was on the fibers. Where a fiber has a spot that is brighter than the immediate area there is comparatively more fluorophore measured, possibly at different focal layer, implying three-dimensional topography.

# Chapter 5. **Discussion**

Electrospun PLCL fibers make a suitable vector for the transport of cells for tissue engineering since the biodegradable polymer will break down and release metabolites into the tissue. The ratio of ε-caprolactone to L-lactide will dictate the degradation profile, allowing the polymer to be tailored to healing time of the application. These electrospun fibers are mostly smooth with some variation depending on the solution used and the geometry of the collector, but the literature mentions that varying the solvents used effects the inherent porosity of the fibers themselves. Figures 4.2 and 4.4 show that stationary collectors create more topography than the mandrel spun polymer of 4.6, however this may be due to inexperience with the electrospinning apparatus, where fluctuating conditions result from a poorly optimised production method. Variation in fiber surface is beneficial for cells, but before plasma treatment uniform samples will behave more predictably when treated, simplifying experimentation.

Judging by the figure series 4.8 - 4.22 increasing the power of atmospheric plasma treatment increases physical signs of damage to the intricate network of the scaffolds. Atmospheric DBD plasma has relatively low gas and electron temperature compared to thermal plasmas (Hong, 2013) but still applies heat to the fibers either by thermal conduction or exothermic reactions, melting the fibers. The fibers are thin so according to the heat flux equation:

$$Q = \frac{k \times A(\Delta T)}{d}$$

Where 'Q' is heat transfer, 'k' is thermal conductivity, 'ΔT' is the difference in temperature between the heat source and sample, and 'A' is the area of the sample of uniform thickness 'd'. More heat is transferred to thin material, thicker samples may resist melting by having more thermal mass to dissipate the heat.

DBD treatment does not affect the bulk properties of the material as evidenced by the unchanged peak positions between graph 2 and 5. Peak position should not shift, since the chain scissions created by the atmospheric plasma will not change the chemistry of the bulk material, and surface grafted hydroxyl groups will not make a significant change to the relative stoichiometry of PLCL ($C_4H_6O_2$). By comparison to the graph obtained by Elzein *et al.*, (2004) the peaks mostly line up, with some discrepancy possibly due to different sourcing and sample chain lengths, the majority of the defining peaks are easily spotted by the active peak finding of KnowItAll FTIR software (Bio-Rad, Berkeley U.S.), and the unidentified peaks could be disguised in overlap.

PCL and PLA, the constituent polymers of PLCL, are U.S. FDA approved for medical devices, this is not a guarantee that this copolymer is also approved however, by proving DBD treatment does not affect the bulk chemistry of the material the treated material would be ratified as well as PLCL.

The contact angle analysis suggests that the 750W treatment increases the hydrophilicity of the samples more than any other, but as described shows too much damage to the fibers. 500W represents a balance between topography and contact angle such that both will play a role in improving cellular interactions.

Experimentation with adhering BSA to the plasma treated scaffolds revealed that the thin material has little to no resistance to rolling into itself, whether this is due to intermolecular forces or if tension remains in the fibres is unknown. To mitigate the scaffold's propensity to fold some part, preferably all, of the edge is trapped beneath a plastic ring as seen in fig 3.1 however, this ring design did not keep the samples flat. The rings are 3D printed in ABS, which has a density of 1.05 $g/cm^3$ meaning when water was introduced during the washing steps, small pockets of air under the scaffolds or in the print had enough buoyancy to cause the ring to dislodge allowing the sample to move and slip out from the under sized internal diameter of the ring. If a sample is left to free-float it will shrivel up and become useless to the experiment, meaning forceps and other tools had to be sterilised and used to gently manipulate the scaffold beneath the ring, depressing and marring in the material.
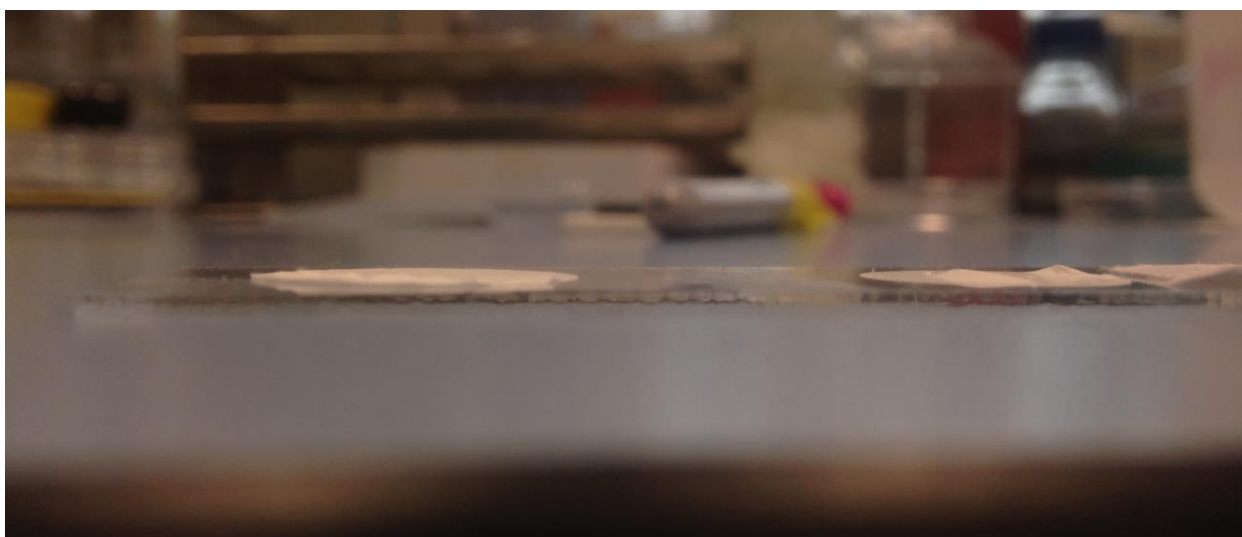
***Figure 5.1*** FBS treated pristine PLCL samples, edges curling and creases form in the material, obscuring the level surface needed by the KSV software to measure the contact angle of the three phase boundaries.

Once dry the samples tend to lay flat on the well plate, but after removal many of the samples had ruffled edges, obscuring the camera for contact analysis see *fig 5.1*. Pressing three of each sample, sandwiched between microscope slides, under a large book overnight. The resulting samples were no more flat, and some had ripples propagating from the mid-point as if bowed, possibly due to the manhandling of the material to tease it from the fin foil after spinning. Additionally, other samples were wetted to attempt to recreate whatever conditions allowed the samples to remain flat after the experiment. There was limited success with this method where crushed folds were cut away with scissors, the samples that had been submerged in FBS were more easily wetted than the control samples, suggesting that there was something adhered to the material that improved its hydrophilicity. However due to difficulties with the samples, no empirical evidence could be gathered.

The SEM figure series 4.22 to 4.27 should show little to no change, FBS is a mixture that is regularly used for *in vitro* cell culture, at lower concentrations like 10-20%, with no damage to the fibers. At higher concentrations of FBS, there would be less water to hydrolytically degrade the material, Gao *et al*., (2018) saw similar degradation of 90/10, PCL /PLGA in lipase over 4 weeks. The paper explains that the acidic metabolites catalyse the hydrolysis of the ester bonds in water, even with the increased hydrophilicity of the DBD treated samples the damage to the fibers would not be that severe after 24 hours. The FBS is unlikely to be a source of active enzymes, since it is heated in a water bath at 50 ºC that would denature mammalian lipase protein.

The only difference between the initial and second experiment was the sterilisation of everything for the first experiment. After the first experiment, sterilisation was considered unnecessary since no cells were seeded onto the sample. This does not rule out the possibility of a foreign body or pathogen getting into the experiment and producing enzymes to degrade the polymer, this is only speculation since the waste FBS was disposed of rather than tested for bacterial DNA using PCR.

Figures 4.29 through to 4.32 exhibit unparalleled damage to the fibers and overall scaffold, fissures that appear in figure 4.29 look almost like stretch marks, it was suggested that the damage was a result of excess handling which may explain the damage. However, this was the only sample that was seen to have this damage, and it happens that this sample had adhered strongly to the well plate. It is possible that the fractures in the material are a result of mechanical forces required to remove it for imaging, this still does not explain the damage to the FBS experiment images that were taken of samples not ripped from the well plate.

Graph 7 shows a difference between the spectra of PLCL that was soaked in water and those that were soaked in FBS. A very weak, very broad peak begins to appear on the middle graph at 3305.42 cm$^{-1}$ that is detected by the software in the top graph. This peak is associated with primary amine groups, since the peak is so small it is possible it is an error, or it could be small because there is a low concentration of amine bonds adhered to the surface of the fibers (Smith, 2015).  If the relative peak height difference is an indication the DBD samples have a higher concentration of FBS, then that would suggest that this technique, with refinement could be used to adhere peptides to electrospun polymers.

Negative control samples (fig 4.32) does not suggest any specific binding, if a negative control is fluorescent, this means the sample is auto-fluorescent or the secondary antibody was not completely removed by the wash step. Bright green fibers in fig 4.35 show unequivocal evidence that BSA binds to DBD treated PLCL fibers, since the primary antibody binds specifically, the fluorescence compared to the control (fig 4.33) show BSA bonding to positive structures in the samples. The faint green of the pristine PLCL fibers (fig 4.34) suggest protein can bind to the surface, and since the LASER settings were the same between 4.35 and 4.34, speculation could be made comparing the binding affinity's but as mentioned, confocal microscopy is not reliable for quantitative analysis without the regular testing of the machine and experimental design outlined by Jonkman, Brown and Cole (2014).

Submerging the scaffolds in excess FBS is not a cost effective method of adsorption, in production, peptides would be dissolved into the serum-free growth medium that would be

cycled through the bioreactor before cell seeding, so that the peptides can adsorb to the scaffolds. Or the peptides would be chemically bonded to the material in a separate process.

Due to time management errors based on an underestimation of the challenges associated with electrospinning production and sample handling, peptide adsorption experiments were delayed. Cancellation extended to RGD experimentation, but revealed there is not enough literature on effective handling and preparation for testing of thin electrospun scaffolds. The adhesion method of 24hr incubation is mentioned by Mahmoudifard *et al.*, (2016) using 250-300 μm scaffolds to avoid the floating issue, which does not solve the issues of developing nano-structures like basement membranes that are 50-100 microns thick (Goodman, 2008) unless layered with calculated spin durations creating multi-layered structures with different properties (Bridge *et al.*, 2015). The composite scaffolds produced by Bridge *et al.* (2015) can be used to mimic the structure and orientation at many layers of tissue for remodelling, but thin individual layers may need to be tested separately to tailor the basal membrane, 40-120 nm, for different tissue types.

# Chapter 6. **Conclusion**

FTIR analysis suggests evidence of the presence of primary amine groups that is not existent on the control analysis. With limited experience with FTIR, relative concentration can be difficult to estimate, but the peak at 3305 cm$^{-1}$ is more pronounced for the DBD treated scaffolds, suggesting there may be improved adsorption. However, the relatively small quantity of peptide that is bonded to the scaffold requires sensitive equipment to quantify it, and establish a minimum effective concentration. There is evidence that the PLCL scaffolds can adsorb peptides to the surface, and that 500W DBD plasma treatment does not stop their adsorption.

Functionalisation by this method requires further optimisation, due to variable results, but boasts a possible method for non-specific peptide adherence that can theoretically be used to design a cellular response *in vitro*, depending on the bio cues adsorbed.

## 6.1   **Further Experimentation**

By changing the parameters of the electrospinning machine, the surface of the fiber can become porous by using highly volatile solvents (Leach *et al.* 2011). Improved topography may improve hydrophilicity of the scaffolds without the need of DBD plasma treatment. Fine features of these fibers may be rounded off by DBD plasma, which may be beneficial or detrimental depending on the cell type chosen.

The Degradation of PLCL fibers in FBS should be further investigated as rapid degradation would not result in effective tissue engineering. Since these scaffolds would be subject to enzymatic and acid catalysed hydrolysis *in vivo* the material must have a predictable degradation profile.

RGD is the bio cue of choice for cellular interaction because it is a very common repeating sequence in extracellular matrix components, meaning if coating the electrospun fibers, the scaffolds would better mimic the ECM. It is associated with undifferentiating cells and so would not cause spontaneous differentiation when the scaffold is seeded, allowing the differentiation to be governed by the other factors involved like mechanotransduction and growth factor presence.

Establishing a method of covalently bonding or polymerising RGD peptides to the material would be a more robust bio cue coating that would better resist hydrolytic degradation. By using the radicals formed in DBD plasma to radicalise amine and carboxyl groups, polymerisation may occur between the peptides, without experimentation it is uncertain what would polymerise. RGD contains two amine and two carboxylic acid groups that could react with each other, never bonding to the surface creating clots of RGD that adhere to the scaffold. Rampant polymerisation could be the result regardless of the polymerisation process without first grafting relevant functional groups that act as an anchor to the scaffold.

Radical production pathways (Wertheimer *et al.*, 1990):

$$RH => R\bullet + H\bullet$$

$$R\bullet + O_2 => ROO\bullet$$

$$ROO\bullet + A => ROOH + \bullet A$$
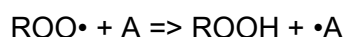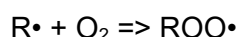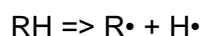
If R is the carbon backbone of one of the PLCL fibers and the A group is an amide group on RGD, the radical termination in atmospheric DBD plasma treatment will result in peptide bonds, a possible method of covalently bonding RGD to PLCL or most carbon-based polymer scaffolds. As well, the cross-linking of RGD tripeptides may stabilise the scaffold to degradation, slowing the release of lactic acid into the surrounding tissue, allowing waste transport so as not to cause acidosis.

Depending on the results of the RGD experiments, to more accurately mimic the ECM, fibronectin and proteoglycan complexes could be adhered to the scaffolds. Fibronogen's wound healing involvement (Goodman 2008) could benefit remodelling *in vivo* from the induced cellular response. Possibly producing the scaffolds using collagen as a natural polymer, for comparison to PLCL spun, to establish if synthetic polymers coated in ECM are a viable competitor for bioengineered extracellular matrix. Fibrinogen contributes to the formation of atheromas on biomedical implants due to the competitive adsorption and desorption described by the Vroman effect presenting fibrinogen ligands to bind to platelet cell's glycoprotein receptors.

# Chapter 7. **Bibliography**

Chauvin, J., Judée, F., Yousfi, M., Vicendo, P. and Merbahi, N. (2017). Analysis of reactive oxygen and nitrogen species generated in three liquid media by low temperature helium plasma jet. *Scientific Reports*, [online] 4562(2017). Available at: https://www.nature.com/articles/s41598-017-04650-4 [Accessed 30 Nov. 2018].

Electrospin Tech (2015, updated 2019). *Influence of fiber alignment on cells and tissue regeneration*. [online] Electrospintech.com. Available at: http://electrospintech.com/cellalignfibers.html#.XJfRFiDgpjU [Accessed 24 Mar. 2019].

Vidya-mitra., (2018). Nanofibers – electrospinning technique [online]. *Youtube.* [Viewed 06 December 2018]. Available at: https://www.youtube.com/watch?v=owpLUPU5ZA4

# Chapter 8. **References**

Alberts, B. (2002). *Molecular biology of the cell*. 4th ed. New York: Garland. Ch 19

Augustine, R., Kalarikkal, N. and Thomas, S. (2015). Effect of zinc oxide nanoparticles on thein vitrodegradation of electrospun polycaprolactone membranes in simulated body fluid. *International Journal of Polymeric Materials and Polymeric Biomaterials*, [online] 65(1), pp.28-37. Available at: https://www.researchgate.net/publication/286926828_In_Vitro_Degradation_of_Electrospun_Polycaprola ctone_Membranes_in_Simulated_Body_Fluid [Accessed 22 Apr. 2019].

Barczyk, M., Carracedo, S. and Gullberg, D. (2009). Integrins. *Cell and Tissue Research*, [online] 339(1), pp.269-280. Available at: https://www.ncbi.nlm.nih.gov/pmc/articles/PMC2784866/ [Accessed 24 Apr. 2019].

Biggs, M., Richards, R., Gadegaard, N., Wilkinson, C., Oreffo, R. and Dalby, M. (2009). The use of nanoscale topography to modulate the dynamics of adhesion formation in primary osteoblasts and

ERK/MAPK signalling in STRO-1+ enriched skeletal stem cells. *Biomaterials*, [online] 30(28), pp.5094-5103. Available at: https://www.sciencedirect.com/science/article/pii/S0142961209005808?via%3Dihub [Accessed 3 May 2019].

Bostwick, J. and Steen, P. (2009). Capillary oscillations of a constrained liquid drop. *Physics of Fluids*, [online] 21(3), p.032108. Available at: https://cecas.clemson.edu/~jbostwi/wp-content/uploads/2017/07/jbbphsPOF2009.pdf [Accessed 6 Apr. 2019].

Boyce, J., Wong, P., Schürch, S. and Roach, M. (1983). Rabbit arterial endothelium and subendothelium. A change in interfacial free energy that may promote initial platelet adhesion. *Circulation Research*, [online] 53(3), pp.372-377. Available at: https://www.ahajournals.org/doi/pdf/10.1161/01.RES.53.3.372 [Accessed 28 Apr. 2019].

Bridge, J., Ayolott, J., Brightling, C., Ghaemmaghami, A., Knox, A., Lewis, M., Rose, F. and Morris, G. (2015). Adapting the Electrospinning Process to Provide Three Unique Environments for a Tri-layered *In Vitro* Model of the Airway Wall. *Journal of Visualized Experiments,* [online] (101), Available at: https://www.ncbi.nlm.nih.gov/pmc/articles/PMC4544510/ [Accessed 24 Mar. 2019].

Christopherson, G., Song, H. and Mao, H. (2009). The influence of fiber diameter of electrospun substrates on neural stem cell differentiation and proliferation. *Biomaterials*, [online] 30(4), pp.556-564. Available at: https://www.sciencedirect.com/science/article/pii/S0142961208007783?via%3Dihub [Accessed 7 Apr. 2019].

Cramariuc, B., Cramariuc, R., Scarlet, R., Manea, L., Lupu, I. and Cramariuc, O. (2013). Fiber diameter in electrospinning process. *Journal of Electrostatics*, [online] 71(3), pp.189-198. Available at: https://www.sciencedirect.com/science/article/pii/S0304388612001726 [Accessed 3 May 2019].

Denchai, A., Tartarini, D. and Mele, E. (2018). Cellular Response to Surface Morphology: Electrospinning and Computational Modeling. *Frontiers in Bioengineering and Biotechnology*, [online] 6(Oct). Available at: https://doi.org/10.3389/fbioe.2018.00155 [Accessed 23 Mar. 2019].

Gao, J., Chen, S., Tang, D., Jiang, L., Shi, J. and Wang, S. (2018). Mechanical Properties and Degradability of Electrospun PCL/PLGA Blended Scaffolds as Vascular Grafts. *Transactions of Tianjin University*, [online] 25(2), pp.152-160. Available at: https://link.springer.com/article/10.1007/s12209-018-0152-8 [Accessed 27 Apr. 2019].

Goodman, S. (2008). *Medical cell biology*. 3rd ed. London: Academic Press, pp.220-221.

Grumezescu, A., Dwivedi, C., Pandey, I., Pandey, H., Ramteke, P., Pandey, A., BhushanMishra, S. and Patil, S. (2017). *Nano- and microscale drug delivery systems, Chapter 9*. 1st ed. Amsterdam: Elsevier, pp.147-164.

Güven, O. (1990). *Crosslinking and scission in polymers*. 2nd ed. Dordrecht: Kluwer Academic Publishers, p.1-13.

Hong, J. (2013). *A TMOSPHERIC PRESSURE PLASMA CHEMICAL DEPOSITION BY USING DIELECTRIC BARRIER DIS CHARGE SYSTEM*. Masters. University of Illinois at Urbana.

Johnson, M. 2012. 'Protein Quantification'. *Labome,* vol 2, no. 115. [online] Available at: https://www.labome.com/method/Protein-Quantitation.html [Accessed 06 Apr. 2019].

Jonkman, J., Brown, C. and Cole, R. (2014). Quantitative confocal microscopy. *Methods in Cell Biology*, [online] 123, pp.113-134. Available at: https://www.sciencedirect.com/science/article/pii/B9780124201385000070 [Accessed 8 May 2019].

Kerr, M. 2011*. 'The Grafting of Collagen to Medically Relavent Polymers through an Atmospheric Pressure Dielectric Barrier Discharge'*. PhD. Ulster University.

Kim, C. (2013). Crawling of effector T cells on extracellular matrix: role of integrins in interstitial migration in inflamed tissues. *Cellular & Molecular Immunology*, [online] 11(1), pp.1-4. Available at: https://www.nature.com/articles/cmi201347 [Accessed 28 Apr. 2019].

Ko, I., Lee, S., Atala, A. and Yoo, J. (2013). In situ tissue regeneration through host stem cell recruitment. *Experimental & Molecular Medicine*, [online] 45(11), pp.e57-e57. Available at: https://www.nature.com/articles/emm2013118 [Accessed 5 May 2019].

Larrañaga, A., Guay-Bégin, A., Chevallier, P., Sabbatier, G., Fernández, J., Laroche, G. and Sarasua, J. (2014). Grafting of a model protein on lactide and caprolactone based biodegradable films for biomedical applications. *Biomatter*, [online] 4(1), p.e27979. Available at: https://www.ncbi.nlm.nih.gov/pmc/articles/PMC4014455/ [Accessed 18 Nov. 2018].

Lauer, J., Shohet, J., Albrecht, R., Esnault, S., Malter, J., von Andrian, U. and Shohet, S. (2005). Control of uniformity of plasma-surface modification inside of small-diameter polyethylene tubing using microplasma diagnostics. *IEEE Transactions on Plasma Science*, [online] 33(2), pp.791-798. Available at: https://www.researchgate.net/publication/3166125_Control_of_uniformity_of_plasma-surface_modification_inside_of_small-diameter_polyethylene_tubing_using_microplasma_diagnostics [Accessed 20 Dec. 2018].

Leach, M., Feng, Z., Tuck, S. and Corey, J. (2011). Electrospinning Fundamentals: Optimizing Solution and Apparatus Parameters. *Journal of Visualized Experiments*, [online] 47(1). Available at: https://www.ncbi.nlm.nih.gov/pmc/articles/PMC3182658/ [Accessed 24 Nov. 2018].

MacDonald, C., Morrow, R., Weiss, A. and Bilek, M. (2008). Covalent attachment of functional protein to polymer surfaces: a novel one-step dry process. *Journal of The Royal Society*, [online] 5(23), pp.663-669. Available at: https://royalsocietypublishing.org/doi/full/10.1098/rsif.2007.1352 [Accessed 18 Dec. 2018].

Mahmoudifard, M., Soleimani, M., Hatamie, S., Zamanlui, S., Ranjbarvan, P., Vossoughi, M. and Hosseinzadeh, S. (2016). The different fate of satellite cells on conductive composite electrospun nanofibers with graphene and graphene oxide nanosheets. *Biomedical Materials*, [online] 11(2), p.025006. Available at: https://iopscience.iop.org/article/10.1088/1748-6041/11/2/025006/meta [Accessed 5 May 2019].

Noriega, S., Hasanova, G., Schneider, M., Larsen, G. and Subramanian, A. (2012). Effect of Fiber Diameter on the Spreading, Proliferation and Differentiation of Chondrocytes on Electrospun Chitosan Matrices. *Cells Tissues Organs*, [online] 195(3), pp.207-221. Available at: https://www.ncbi.nlm.nih.gov/pmc/articles/PMC3697793/ [Accessed 6 May 2019].

Payton, O., Champneys, A., Homer, M., Picco, L. and Miles, M. (2010). Feedback-induced instability in tapping mode atomic force microscopy: theory and experiment. *Proceedings of the Royal Society A: Mathematical, Physical and Engineering Sciences*, [online] 467(2130), pp.1801-1822. Available at: https://royalsocietypublishing.org/doi/full/10.1098/rspa.2010.0451 [Accessed 6 Apr. 2019].

Payan, Y. and Ohayon, J. (2017). *Biomechanics of Living Organs*. 1st ed. Academic Press, pp.565-575.

Pease, L., Elliott, J., Tsai, D., Zachariah, M. and Tarlov, M. (2008). Determination of protein aggregation with differential mobility analysis: Application to IgG antibody. *Biotechnology and Bioengineering*, [online] 101(6), pp.1214-1222. Available at: https://onlinelibrary.wiley.com/doi/epdf/10.1002/bit.22017 [Accessed 27 Apr. 2019].

Pham, Q., Sharma, U. and Mikos, A. (2006). Electrospinning of Polymeric Nanofibers for Tissue Engineering Applications: A Review. *TISSUE ENGINEERING*, [online] 12(5). Available at: https://pdfs.semanticscholar.org/5beb/3ffe0db48d87505076ae044eafd87749b7eb.pdf [Accessed 6 Mar. 2019].

Pretorius, E. (2009). Influence of acceleration voltage on scanning electron microscopy of human blood platelets. *Microscopy Research and Technique*, [online] 73, pp.225-228. Available at: https://onlinelibrary.wiley.com/doi/pdf/10.1002/jemt.20778 [Accessed 28 Apr. 2019].

Rehman, M., Jawaid, P., Uchiyama, H. and Kondo, T. (2016). Comparison of free radicals formation induced by cold atmospheric plasma, ultrasound, and ionizing radiation. *Archives of Biochemistry and Biophysics*, [online] 605(September), pp.19-25. Available at: https://www.sciencedirect.com/science/article/pii/S0003986116301151 [Accessed 30 Nov. 2018].

Royal Society of Chemistry (2009). *Spectroscopy in a Suitcase students' resource: Infrared spectroscopy*. [PDF] London: Royal Society of Chemistry. Available at: http://www.rsc.org/learn-chemistry/resource/res00000283/spectroscopy-in-a-suitcase-ir-student-resources [Accessed 15 Dec. 2018].

Shen, X., Ma, P., Hu, Y., Xu, G., Zhou, J. and Cai, K. (2015). Mesenchymal stem cell growth behavior on micro/nano hierarchical surfaces of titanium substrates. *Colloids and Surfaces B: Biointerfaces*, [online] 127(3), pp.221-232. Available at: https://www.sciencedirect.com/science/article/pii/S0927776515000648?via%3Dihub [Accessed 3 May 2019].

Shoulders, M. and Raines, R. (2009). Collagen Structure and Stability. *Annual Review of Biochemistry*, [online] 78(1), pp.929-958. Available at: https://www.ncbi.nlm.nih.gov/pmc/articles/PMC2846778/ [Accessed 3 May 2019].

Sirsi, S. 2014. *How can I quantify an RGD peptide covalently bound onto polymeric nanoparticle surface?* [Research Gate Forum] April 2014. Available at: https://www.researchgate.net/post/How_can_I_quantify_an_RGD_peptide_covalently_bound_onto_polymeric_nanoparticle_surface [Accessed 18th December 2018].

Smith, B. (2015). *IR Spectral Interpretation Workshop*. [online] SpectroscopyOnline. Available at: http://www.spectroscopyonline.com/ir-spectral-interpretation-workshop?pageID=1 [Accessed 3 May 2019].

Song, J., Sun, B., Liu, S., Chen, W., Zhang, Y., Wang, C., Mo, X., Che, J., Ouyang, Y., Yuan, W. and Fan, C. (2016). Polymerizing Pyrrole Coated Poly (l-lactic acid-co-ε-caprolactone) (PLCL) Conductive Nanofibrous Conduit Combined with Electric Stimulation for Long-Range Peripheral Nerve Regeneration. *Frontiers in Molecular Neuroscience*, [online] 9(117). Available at: https://www.frontiersin.org/articles/10.3389/fnmol.2016.00117/full [Accessed 29 Apr. 2019].

Tallawi, M., Rosellini, E., Barbani, N., Cascone, M., Rai, R., Saint-Pierre, G. and Boccaccini, A. (2015). Strategies for the chemical and biological functionalization of scaffolds for cardiac tissue engineering: a review. *Journal of The Royal Society Interface*, [online] 12(108), p.20150254. Available at: https://www.ncbi.nlm.nih.gov/pmc/articles/PMC4528590/?fbclid=IwAR2eIJMnGuQm1-ZtBuat-kzffKu23Ku-hvkyO06CbTXKDp1Q82Z9Nyj4Akw [Accessed 30 Oct. 2018].

Tran, T., Ens-Blackie, K., Rector, E., Stelmack, G., McNeill, K., Tarone, G., Gerthoffer, W., Unruh, H. and Halayko, A. (2007). Laminin-Binding Integrin α7 Is Required for Contractile Phenotype Expression by Human Airway Myocytes. *American Journal of Respiratory Cell and Molecular Biology*, [online] 37(6), pp.668-680. Available at: https://www.atsjournals.org/doi/full/10.1165/rcmb.2007-0165OC [Accessed 5 May 2019].

van der Valk, J., Bieback, K., Buta, C., Cochrane, B., Dirks, W., Fu, J., Hickman, J., Hohensee, C., Kolar, R., Liebsch, M., Pistollato, F., Schulz, M., Thieme, D., Weber, T., Wiest, J., Winkler, S. and Gstraunthaler, G. (2018). Fetal bovine serum (FBS): Past – present – future. *ALTEX*, [online] 35(1), pp.99-118. Available at: https://www.ncbi.nlm.nih.gov/pubmed/28800376 [Accessed 6 May 2019].

Varesano, A. (2015). *Introduction to electrospinning* [Portable Document Format]. Unknown. Available at: https://www.2bfuntex.eu/sites/default/files/materials/Introduction%20to%20electrospinning.pdf [Accessed 09 December 2018].

Wertheimer, M., Fozza, A. and Holländer, A. (1999). Industrial processing of polymers by low-pressure plasmas: the role of VUV radiation. *Nuclear Instruments and Methods in Physics Research Section B: Beam Interactions with Materials and Atoms*, [online] 151(1-4), pp.65-75. Available at: https://www.researchgate.net/publication/223235493_Industrial_processing_of_polymers_by_low-pressure_plasmas_The_role_of_VUV_radiation [Accessed 20 Dec. 2018].

Xu, J., Zhang, C., Shao, T., Fang, Z. and Yan, P. (2013). Formation of hydrophobic coating on PMMA surface using unipolar nanosecond-pulse DBD in atmospheric air. *Journal of Electrostatics*, [online] 71(3), pp.435-439. Available at: https://gd2014.sciencesconf.org/28549/document [Accessed 2 May 2019].

**Appendix A. Electrospinning COSHH ASSESSMENT
RA3**

| School | Engineering | Assess. No. | 01 |
|---|---|---|---|
| Title of Activity | Electrospinning | | |
| Location(s) of Work | NIBEC | | |

Outline of task/method: Deposition of poly(L-Lactide-co-ε-caprolactone (PLCL) on a piece of glass, the PLCL is dissolved in chloroform and N,N-Dimethylformamide. The PLCL solution is deposited across a short distance between a high voltage, in a fume hood. ATR-FTIR characterisation

# A. Hazards including any substances produced during the procedure

| Name of substance(s) and classify hazard | Toxic or Very Toxic | Irritant | Oxidizing | Corrosive | Flammable | Dangerous for the Environment | Health hazzard | Explosive | Gas Pressure |
|---|---|---|---|---|---|---|---|---|---|
| PLC | No | No | No | No | No | No | No | No | No |
| Chloroform | Toxic | Yes | No | No | No | Yes | Yes | No | No |
| FBS | No | No | No | No | No | No | No | No | No |
| DMF | No | Yes | No | No | Yes | Yes | Yes | No | No |
| Nitrogen (liquid) | No | No | No | No | No | No | No | No | Yes |
| | | | | | | | | | |

## B. Exposure route(s) by which harm may occur

| Substance(s) | Skin Contact | Skin Absorption | Eye Contact | Inhalation | Ingestion | Injection via sharps |
|---|---|---|---|---|---|---|
| Chloroform | Yes | Yes | Yes | Yes | Yes | Yes |
| DMF | No | No | Yes | Yes | Yes | Yes |

| | | | | | | |
|---|---|---|---|---|---|---|
| PLCL | No | No | No | No | No | No |
| FBS | No | No | No | No | No | No |
| Nitrogen (l) | Yes | No | Yes | Yes | No | No |

## 8.1.2 C. Engineering Control Measures (Fume cupboards/LEV etc.)

Keep chloroform and DMF under a fume hood, and the cap sealed tightly. Where Viton gloves when handling chloroform and DMF. Keep DMF away from sources of ignition, sparks and open flames.

Provide adequate ventilation for liquid nitrogen.

## 8.1.3 D. Personal Protective Equipment (PPE)

| State any PPE required for this task/method. Include which type and when they are to be worn; | | | |
|---|---|---|---|
| ☐ Dust mask | | ☐ Visor | Face shield that are EN 166 approved |
| ☐ Respirator | ABEK (EN 14387) respirator cartridges as a backup to engineering controls.. | ☐ Goggles | EN 166 approved Safety Glasses |
| ☐ Gloves | >0.8mm Viton gloves EN 374 Cold insulating gloves | ☐ Overalls | Anti-static lab coat |
| ☐ Footwear | | ☐ Other | |

# E. Health Monitoring

| Is biological monitoring required to ensure that the control of exposure to the hazardous substance(s) is adequate? | 8.1.4 Yes | (8.1)5 No |
|---|---|---|
| Is health surveillance required for the protection of the health of employees? | 8.1.6 Yes | (8.1)7 No |

If yes for health monitoring, arrange an appointment with Occupational Health

# F. Training

State any health and safety training required for this task/method;

Hazard information, spillage training and knowledge of evacuation routes.

# G. Storage

State any requirements for storage areas and containers; under dry Nitrogen, in a sealed, glass container in a well-ventilated space away from oxidising agents, moist air and ignition sources. Keep liquid nitrogen in insulated container.

# H. Supervision

State what supervision (if any) is required for persons undertaking this task; Not required, but the presence of a trained supervisor would be advised for the first few operations to ensure safe practices are used.

# I. Implications for persons not involved in the work activity

Note any persons who may require to be informed, in part or in full, of the information contained in this assessment. Fellow final year project students, masters and PhD students as well as anyone near the electrospinning labs.

# J. Accidental release measures and Waste disposal

For accidental releases define

| Personal precautions | PPE |
|---|---|
| Environmental precautions | Keep DMF and Chloroform under fume hood and tightly sealed when not in use, if there is a fire or spillage, leave calmly via Emergency exit route. |
| Methods for cleaning up | Dry sand or earth |
| State waste disposal routes for all hazardous substances in this task/method; Chemical incineration, or removal of dry sand in a sealed container | |

- Personal precautions i.e. Consider PPE, ventilation, fire/explosion, evacuation requirements
- Environmental precautions
- Methods for cleaning up

## Appendix B. DBD and Peptide Functionalisation COSHH ASSESSMENT
### RA3

| School | ⟦Engineering⟧ | Assess. No. | 02 |
|---|---|---|---|
| Title of Activity | Plasma Treatment and Peptide Functionalisation | | |
| Location(s) of Work | NIBEC | | |

Outline of task/method: Dielectric barrier discharge plasma treatment of electrospun polymers with Foetal Bovine Serum and Arginylglycylaspartic acid (RGD) under oxygen.

# A. Hazards including any substances produced during the procedure

| Name of substance(s) and classify hazard | Toxic or Very Toxic | Irritant | Oxidizing | Corrosive | Flammable | Dangerous for the Environment | Health hazzard | Explosive | Gas Pressure |
|---|---|---|---|---|---|---|---|---|---|
| Ozone/ $O_2$ | No | No | Yes | No | Supports | No | No | Possible | Yes |

| | | | | | | | | |
|---|---|---|---|---|---|---|---|---|
| Amonia/ Ammonium | Yes | Yes | No | Yes | Yes | Yes | Yes | Yes | Yes |
| RGD | No | No | No | No | No | No | No | No | No |
| FBS | No | No | No | No | No | No | No | No | No |
| | | | | | | | | | |

## B. Exposure route(s) by which harm may occur

| Substance(s) | Skin Contact | Skin Absorption | Eye Contact | Inhalation | Ingestion | Injection via sharps |
|---|---|---|---|---|---|---|
| Oxygen | No | No | No | No | No | No |
| Ammonia | Yes | No | Yes | Yes | Yes | No |
| RGD | No | No | No | No | No | No |
| FBS | No | No | No | No | No | No |

## C. Engineering Control Measures (Fume cupboards/LEV etc.)

State any engineering controls required for this task/method;

Appropriate gas cylinders and valves, respiration masks should be worn when using Ammonia. Seals on machines should be checked by a qualified inspector.

## D. Personal Protective Equipment (PPE)

State any PPE required for this task/method. Include which type and when they are to be worn;

| | | | |
|---|---|---|---|
| Dust mask | | ☐ Visor | |
| ☐ | EN 14387 approved filter K respirator | ☐ | |

| | | Goggles | |
|---|---|---|---|
| Respirator | | | |
| ☐ <br><br> Gloves | Chloroprene 0.7mm gloves | ☐ <br><br> Overalls | Flame retardant, and chemically resistant lab coat. |
| ☐ <br><br> Footwear | Safety shoes when handling containers | ☐ <br><br> Other | |

# E. Health Monitoring

| | |
|---|---|
| Is biological monitoring required to ensure that the control of exposure to the hazardous substance(s) is adequate? | (Yes) No |
| Is health surveillance required for the protection of the health of employees? | (Yes) No |

If yes for health monitoring, arrange an appointment with Occupational Health

## F. Training

State any health and safety training required for this task/method; Gas pressure and breathing apparatus training. As well as understanding the toxicity hazard: category 3 inhalation and category 1/1B for eye and skin corrosion.

## G. Storage

State any requirements for storage areas and containers; Gas canisters. ammonia: away from Vitol, copper, tin, zinc and mercury and oxidants including oxygen gas. Refrigerate (4⁰C) or freeze (-25⁰C) FBS

## H. Supervision

State what supervision (if any) is required for persons undertaking this task; only experienced and trained individuals may handle substances under gas pressure

# I. Implications for persons not involved in the work activity

Note any persons who may require to be informed, in part or in full, of the information contained in this assessment. Ammonia leakage could cause damage to persons in the area as well a risk of explosion. Everyone in the vicinity and builing should be aware of this risk, and signage would be required to indicate the dangers of ignition sources near the containers.

## J. Accidental release measures and Waste disposal

For accidental releases define

- Personal precautions i.e. Consider PPE, ventilation, fire/explosion, evacuation requirements
- Environmental precautions
- Methods for cleaning up

| | |
|---|---|
| Personal precautions | PPE, do not discharge ammonia to atmosphere |
| Environmental precautions | Remove all ignition sources |
| Methods for cleaning up | Turn on 2A or 2B scrubber, a gentle mist of water should be dispersed and leave area calmly preferably wearing a respirator. |

State waste disposal routes for all hazardous substances in this task/method;

EIGA discharge into scrubber 2A or 2B

**If in doubt contact the University Sustainability Manager**

| Are you satisfied that the control measures outlined above are adequate to control the risks to health from the hazardous substances used in the work activity described to the lowest level reasonably practicable? **If no, work cannot continue until safe to do so** | **8.1.8 Yes** | **8.1.9 No** |
|---|---|---|

## Abstract C

## Electrospinning

Equipment

- Horizontal electrospinner (IME, Siemens control panel)
- Solution pump (Aladdin programmable syringe pump AL-1000)
- Rotating mandrel (Diameter 75mm, length 164mm )
- Gold / Palladium Sputter Coater (Emitech K650X)
- Scanning Electron Microscope (SEM) (JOEL JSM-6010PLUS/LV)
- ATR FTIR spectrometer (Varian 610-IR)

- PLCL 70/30, Mw ≈ 202,000 g/mol (from Corbin)
- 3 mL syringes (? )
- 18, 20, 21 gauge needles, 21 g not sharp.
- 300 mm lengths of Diba Omnifit® PTFE tubing ID: 0.8mm
- Tube to needle adapter
- Anti-Static cleaning foam spray (RS132-526)
- Tin foil strips (300x60mm)

Method

- Formulate a 10% by weight PLCL solution with a solvent ratio of 8:2, chloroform to DMF. Mix thoroughly overnight to fully homogenise the solution.
- Initiate electrospinning between 16 and 12 kilovolts (kV), with a solution pump rate of 2.00 millilitres per hour (mL/hr).
- Slowly extract the (recently mixed) solution into a 3mL syringe using an 18 gauge (g) needle, remove any bubbles in the syringe by holding it upright and flicking the body.
- Remove the 18 g needle and replace it with a 20 g needle.
- Insert the 20 g needle into one end of the PTFE tube, and after threading through the electrospinning chamber port, insert the spinning needle adapter into the other end of the tubing.
- Place a 21 gauge spinning needle onto the adapter and secure it at the positive electrode, measuring 15 cm between the needle tip and the grounded rotating mandrel at 2.5 V.
- "Purge" the syringe by pumping the solution through the tube until it forms a bead at the needle tip, wipe the tip until the bead stops forming.
- Cover sides of the mandrel with paper to narrow the collection area and clean the chamber with anti-static cleaner foam spray.
- Secure a 60 mm by 300 mm strip of tin foil around of the mandrel tape, for easy removal of the sample.
- Start the electrospinner and pump once the door is closed, and watch the needle tip, if the Taylor cone grows too large or becomes asymmetrical, turn off the pump and wipe the needle tip, close the machine and resume the pump.

- Run machine until 2.0 mL of solution is dispensed onto the foil, whipping the needle tip when the Taylor cone becomes asymmetrical then remove the sample for inspection of thickness.
- Gold coat the first viable sample under vacuum, and inspect it with an SEM at 15mm offset, 40 – 50 spot size, 5 - 10kV.
- If samples are 20 μm thick and the fibers are randomly aligned and between 1.0 - 2.0 μm in diameter, continue spinning as many samples as is needed
- FTIR a sample to determine if there are left-over solvent residues that could damage patients.


## Plasma treatment

Equipment

- DBD plasma machine (Arcotec Coronagenerator)
- Contact angle camera (KSV Cam 200 optical contact angle)

- Glass slides (S8902-1PAK)
- Insulating Tape (RS 408-9451)
- 0.5 - 10μL Adjustable pipette (Genex Beta, 1.5% inaccuracy at 5 μL (±75nL))
- 10μL Pipette tip (Finntip-94052000)
- Glycerol (MFCD00004722)


Method

- Carefully peel the scaffold away from the tin foil and place on a slide, being sure to replace the bottom layer so that it lays on the slide and release tension when pressing the material to the glass.
- Tape the sides of the samples to the rubber carriage in the DBD machine, to keep the samples flat and thus at the same height from the electrodes.
- Set the power knob depending on the desired power level to be applied; 250W - 4, 500W – 5.75, 750W – 6.75, 1000W – 8.25 for ten cycles at 20% speed, 740mm from the electrodes.
- Use contact angle measurement to establish the hydrophilicity of the treated surface.
- SEM the scaffolds to statistically analyse the damage to fibers, like thinning and melting, which would reduce the mechanical properties of the mesh and decrease the available surface area for cellular proliferation.

Contact angle Methodology

- Pipette 5 μL of glycerol onto the scaffold surface at the focal length of the camera.
- Record the droplet for 15 seconds as it stabilises on the surface, or as the time point to test wicking.
- Measure Young's contact angle between the three phases and record the left and right angles.
- Find the calculated circles interaction with the surface for a corroborating trend

- Repeat this step in triplicate for each sample to produce a box plot of the contact angles.

## Peptide adherence

Equipment

- Fume hood (LABCLAIRE Aura 550L)
- Astec Microflow – class 2, advanced biosafety cabinet
- Incubator (Sanyo MC0-18AIC)

- 1000µL pipette and tips (Genex Beta)
- A sterile twelve-well plate
- 12 sterilised well rings
- 10mL heat inactivated Foetal Bovine Serum (FBS) (Gibco)

Method

- DBD treat 1/3$^{rd}$ of the scaffolds at 500W to oxidise the surface and improve their hydrophilicity, to increase adsorption of protein to the fibers.
- Sandwich the samples between 2 pieces of paper and cut out 19 mm disks of the PLCL mesh and the DBD treated samples.
- Sterilise the rings and forceps in IMS, and rinse in di-ionised water.
- Place control PLCL scaffold disks in row A of a twelve-well plate, native PLCL scaffolds for FBS in row B and DBD treated scaffolds in row C, with rings to keep the samples flat and at the bottom of the well.
- ==Sterilise the scaffolds in an alcohol series of 10%, 25%, 50%, 70% and 75% IMS to reduce shrinkage, leave the scaffolds in alcohol under a fume hood until ready for use.==
- Wash scaffolds in deionised water three times for 5 minutes to clean the samples of IMS in a sterile fume hood, holding the rings down with the forceps, so the PLCL meshes don't move.
- Pipette 1 mL of FBS into the scaffold wells B and C to fully submerging the samples.
- Incubate the samples at 37 ºC
- Wash the scaffolds to remove any un-adhered FBS for 5 minutes in 3 deionised water washes, and remove as much of the DI water from the wells as possible.
- Dry samples for two days in air.
- Compare the contact angle of each scaffold.
- Measure the IR spectrum of the samples to qualify the adherence of protein to the DBD treated surface.
- Examine the micro-topography of the treated fibers under SEM at 5 kV.

## Immunocytochemistry

Equipment

- Upright confocal microscope (Ziess LSM 5 Passcal)
- 63x /1.4 Oil Objective lense (Ziess C Plan-Apochromat)

- Mouse anti-BSA monoclonal IgG (Santa Cruz Biotechnology Sc-32816)
- Pipettes (Gilson P20 and P1000)
- 1.5 mL Eppendorfs (Thermo Fisher AM12400)

- Molecular water (Thermo Fisher AM9932)
- Rabbit anti-mouse polyclonal IgG, Alexa Fluor 488 (Thermo Fisher A-11059)
- Glass slides
- Glycerol (Sigma Aldrich G5516-500ML)
- Cover slip (Thermo Fisher 18X18-1)
- Immersion Oil (Fisher scientific 12-070-397)

Method

- Incubate negative control and control scaffolds in deionised water, as well as PLCL and DBD treated scaffolds in FBS over 24 hours at 37 ºC.
- Wash the samples 3 x 5 minutes in deionised water to remove loosely bound molecules, and incubate in water overnight to keep samples moist.
- Add 20 µL of primary mouse anti-BSA antibody into 1mL of molecular grade water in a 1.5mL (3.92µg/mL) Eppendorf and divide the solution amongst the samples and store away from light for 60 minutes.
- Rewash the samples three times for 5 minutes to remove unbound antibodies.
- Add 5µL of secondary rabbit anti-mouse IgG antibody conjugated to Alexafluor 488 tag into 1mL of molecular water (9.95µg/mL) and divide solutions between the samples storing them away from light for three hours at most, to avoid background flourescence.
- And again wash the samples three times for 5 minutes in deionised water.
- Place a sample onto a microscope slide and drop 90% glycerol into the middle of the scaffolds and upturn the slide, gently adhere the glycerol to a coverslip ensuring no bubbles are trapped under the glass.
- Seal the microscope slides with a minimal amount of clear nail varnish around the perimeter of the coverslip, to keep the antibodies moist.
- Find a layer in a sample (DBD + FBS) that gives a clear image of fibers, drop immersion oil onto the cover slip and change to the x63 objective lens.
- Optimise the Argon LASER gain and noise to obtain a high resolution image of the fibers and store it.
- Re-use the LASER settings to obtain images of all the samples, for fair comparison of fluorescence.